UNIST

ULSAN NATIONAL INSTITUTE OF
SCIENCE AND TECHNOLOGY

Master's Thesis

Seasonal variation, source identification, and health risk assessment of atmospheric polycyclic aromatic hydrocarbons (PAHs) in Ulsan, South Korea

Na Ra Youn

Department of Urban and Environmental Engineering
(Environmental Science and Engineering)

Graduate School of UNIST

2020

Seasonal variation, source identification, and health risk assessment of atmospheric polycyclic aromatic hydrocarbons (PAHs) in Ulsan, South Korea

Na Ra Youn

Department of Urban and Environmental Engineering

(Environmental Science and Engineering)

Graduate School of UNIST

Seasonal variation, source identification, and health risk assessment of atmospheric polycyclic aromatic hydrocarbons (PAHs) in Ulsan, South Korea

A thesis

submitted to the Graduate School of UNIST

in partial fulfillment of the

requirements for the degree of

Master of Science

Na Ra Youn

07. 07. 2020 Month/Day/Year of submission

Approved by

_____

Advisor

Sung-Deuk Choi

Seasonal variation, source identification, and health risk assessment of atmospheric polycyclic aromatic hydrocarbons (PAHs) in Ulsan, South Korea

Na Ra Youn

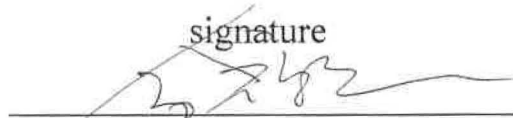This certifies that the thesis of Na Ra Youn is approved.

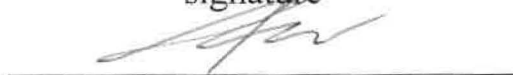07. 07. 2020 Month/Day/Year of submission

signature

_____
Advisor: Sung-Deuk Choi

signature

_____
Chang-Keun Song: Thesis Committee Member #1

signature

_____
Sang Seo Park: Thesis Committee Member #2

Abstract

Polycyclic aromatic hydrocarbons (PAHs) are well-known contaminants due to their toxicity and high emission from incomplete combustion of organic materials. Previous studies mostly focused on the United States Environment Protection Agency priority 16 PAHs; however, other more toxic PAHs have been also found in ambient air (i.e., dibenz[a,i]pyrene (DbaiP), dibenz[a,h]pyrene (DbahP), and dibenz[a,l]pyrene (DbalP)). In this study, gaseous and particulate phases of 21 atmospheric PAHs were collected in three seasons (December 2013–August 2014) at a residential site in Ulsan, South Korea. The samples (n=64) were extracted by Soxhlet extractors, cleaned up using silica gel columns, and then analyzed using a gas chromatograph/mass spectrometer (GC/MS).

The mean Σ_{21} PAH concentrations were 13.06 ng/m^3, 7.67 ng/m^3, and 6.03 ng/m^3 in winter, spring, and summer, respectively. The gaseous concentrations of Σ_{21} PAHs (mean: 7.39 ng/m^3) were higher than the particulate ones (mean: 2.70 ng/m^3). The contribution of the Σ_8 PAHs which are not listed as the US EPA priority PAHs to the Σ_{21} PAH were 5.21%, and they were mostly partitioned in the particulate phase. The particulate PAHs (4-, 5-, and 6-ring species) were dominant in winter, whereas the gaseous PAHs (3- and 4-ring species) were dominant in summer.

In order to identify the emission sources of PAHs, diagnostic ratios, principle component analysis, and a hybrid receptor model (i.e., concentration weighted trajectory) were used. As a result, pyrogenic sources (e.g., wood/coal and natural gas combustion) were the primary sources in winter. Petrogenic sources and petrogenic combustion were dominant in summer, reflecting that PAHs could be transported from industrial areas by seasonal winds. In spring, PAHs were emitted by both petrogenic and pyrogenic sources. In addition, PAHs could be affected by vehicle emission in all seasons. Moreover, the concentration weighted trajectory revealed that PAHs in winter and spring could be contributed by PAHs emitted from regional areas (i.e., China and North Korea).

The exposure-risk probability distribution calculated using Monte Carlo simulation suggested that the cancer risks of Σ_{21} PAHs and Σ_{13} PAHs did not exceed the guideline of the US EPA (10^{-6}). However, high TEFs of DbaiP and DbahP contributed to the increased cancer risk of Σ_{21} PAHs than that of Σ_{13} PAHs although they showed low concentrations in the ambient air. Therefore, it is necessary to investigate for various kinds of PAHs and evaluate their health impact. This is a preliminary study for monitoring and health risk assessment of 21 PAHs in South Korea.

Contents

List of Figures

List of Tables

I. INTRODUCTION

Polycyclic aromatic hydrocarbons (PAHs), a group of chemicals that have two or more benzene rings constituted of carbon and hydrogen in their structure, have been extensively studied due to their potential carcinogenic, teratogenic, and mutagenic properties (IARC, 2004; 2010). Based on their carcinogenicity and mutagenicity, there are 16 species of PAHs have been classified by the United States Environment Protection Agency as priority pollutants: naphthalene (Nap), acenaphthylene (Acy), acenaphthene (Ace), fluorene (Flu), phenanthrene (Phe), anthracene (Ant), fluoranthene (Flt), pyrene (Pyr), benzo[a]anthracene (BaA), chrysene (Chr), benzo[b]fluoranthene (BbF), benzo[k]fluoranthene (BkF), benzo[a]pyrene (BaP), indeno[1,2,3-c,d]pyrene (Ind), dibenzo[a,h]anthracene (DahA), benzo[g,h,i]perylene (BghiP). Among these US EPA 16 priority PAHs, the International Agency for Research on Cancer (IARC) considers BaP a carcinogen to humans (group 1) and BaA and DahA probable carcinogens to humans (group 2A) (IARC, 2010; 2012). However, hundreds of other PAHs as well as these US EPA 16 priority PAHs exist in the environment, and some of them have higher toxicity levels than those of the priority PAHs. For example, dibenz[a,l]pyrene (DbalP) is classified into group 2A. Also, benzo[c]phenanthrene (BcPhe), benzo[j[fluoranthene (BjF), dibenz[a,i]pyrene (DbaiP), and dibenz[a,h]pyrene (DbahP) are classified into a group of possibly carcinogen to human (group 2B). 21 PAHs including the US EPA 13 priority PAHs investigated in this study are shown in Figure 1.

To estimate the detrimental health effects of a mixture of chemicals that have similar structure, the toxicity equivalency factor (TEF) methodology was developed by US EPA and adapted for PAH compounds (Nisbet and Lagoy, 1992; US-EPA, 1993). TEF presents the relative toxicity of individual PAH compounds compared to BaP, which has been well characterized toxicologically (Table 1). The evaluation of toxicity for US EPA priority PAHs are well established, while studies for other PAH compounds are very limited (Andersson and Achten, 2015). For example, DbalP, DbaiP, DbahP are 10 times more carcinogenic than BaP (Andersson and Achten, 2015; OEHHA, 1994), but only DbalP is classified into group 2A. In the cases of 7,12-Dimethylbenz[a]anthracene (DMBA) and 3-Methylcholanthrene (3MCA), they have expected potencies 21.8 and 1.9 times greater in laboratory animals than BaP (Collins et al., 1998; OEHHA, 1994) even though they are no classified in the IARC. In particular, DMBA and 3MCA is widely used to control cancer in laboratory experiments.

Fluorene   Phenanthrene   Anthracene   Fluoranthene

Pyrene   Benzo[c]phenanthrene   Benzo[a]anthracene   Chrysene

Benzo[b]fluoranthene   Benzo[j]fluoranthene   Benzo[k]fluoranthene   7,12-Dimethylbenz[a]anthracene

Benzo[e]pyrene   Benzo[a]pyrene   3-Methylcholanthrene   Indeno[1,2,3-c,d]pyrene

Dibenzo[a,h]anthracene   Benzo[g,h,i]perylene   Dibenzo[a,l]pyrene   Dibenzo[a,i]pyrene

Dibenzo[a,h]pyrene

Figure 1. Chemical structures of the PAHs investigated in this study.

Table 1. Name, abbreviation, IARC classification, and TEF values of 21 PAHs.

Compound	Abbreviation	IARC Classification*[a]	TEF
Fluorene**	Flu	3	0.001[c]
Phenanthrene**	Phe	3	0.001[c]
Antracene**	Ant	3	0.01[c]
Fluoranthene**	Flt	3	0.001[c]
Pyrene**	Pyr	3	0.001[c]
Benzo[c]phenanthrene	BcPhe	2B	-[c]
Banz[a]anthracene**	BaA	2B	0.1[c, d]
Chrysene**	Chr	2B	0.01[c, d]
Benzo[b]fluoranthene**	BbF	2B	0.1[c, d]
Benzo[j]fluoranthene	BjF	2B	0.1[d]
Benzo[k]fluoranthene**	BkF	2B	0.1[c, d]
7,12-Dimethylbenz[a]anthracene	DMBA	-	21.8*[d]
Benzo[e]pyrene	BeP	3	-[c]
Benzo[a]pyrene**	BaP	1[b]	1[c, d]
3-Methylcholanthrene	3MCA	-	1.9*[d]
Indeno[1,2,3-cd]pyrene**	Ind	2B	0.1[c, d]
Dibenz[a,h]anthracene**	DahA	2A	1[c]
Benzo[g,h,i]perylene**	BghiP	3	0.01[c]
Dibenz[a,i]pyrene	DbaiP	2B	10[d]
Dibenz[a,h]pyrene	DbahP	2B	10[d]
Dibenz[a,l]pyrene	DbalP	2A	10[d]

*Classification system: Group 1: carcinogenic to humans, Group 2A: Probably carcinogenic to humans, Group 2B: Possibly carcinogenic to humans, Group 3: Not classifiable as to its to humans

**US EPA 13 priority PAHs

[a] (IARC, 2010)

[b] (IARC, 2012)

[c] (Nisbet and Lagoy, 1992)

[d] (OEHHA, 1994)

The PAHs are produced by natural processes such as forest fire and volcanic eruptions. However, the majority of these pollutants are anthropogenic process: coal and biomass burning, oil and natural gas combustion, and industrial processes (Mostert et al., 2010). Also, PAHs are emitted from petrogenic sources such as oil spillages or leakages (da Silva and Bícego, 2010). Each PAH in the atmosphere behaves differently due to its different physicochemical properties. The low-molecular weight PAHs which consist of 2- or 3- benzene rings, tend to exist in the gaseous phase because they have a high vapor pressure, whereas the high-molecular weight PAHs, which contain 5- or 6- rings, tend to bind to particles in the atmosphere. The physicochemical properties (i.e., formula, molecular weight, water solubility, vapor pressure, octanol/water partition coefficient (K_{OW})) are shown in Table 2.

Table 2. Physiochemical properties including formula, molecular weight, vapor pressure, water solubility, and Log K_{OW} of the target PAHs at 25 °C (Mackay et al., 2006a).

Compound	CAS No.	Abbrev.	Formula	Molecular weight (g/mol)	Vapor pressure (mmHg)	Water solubility (mg/L)	Log Kow
Fluorene	86-73-7	Flu	C13H10	166.2185	6.E-04	1.9	4.18
Phenanthrene	85-01-8	Phe	C14H10	178.2292	1.E-04	4.57	4.46
Antracene	120-12-7	Ant	C14H10	178.2292	6.E-06	0.045	4.63
Fluoranthene	206-44-0	Flt	C16H10	202.2506	9.E-06	0.26	4.85
Pyrene	129-00-0	Pyr	C16H10	202.2506	5.E-06	0.132	4.9
Benzo[c]phenanthrene	195-19-7	BcPhe	C18H12	228.2879			
Banz[a]anthracene	56-55-3	BaA	C18H12	228.2879	2.E-07	0.011	5.61
Chrysene	218-01-9	Chr	C18H12	228.2879	6.E-09	0.0015	5.73
Benzo[b]fluoranthene	205-99-2	BbF	C20H12	252.3093	5.E-07	0.0015	5.78
Benzo[j]fluoranthene	205-82-3	BjF	C20H12	252.3093		0.0025	0.0099
Benzo[k]fluoranthene	207-08-9	BkF	C20H12	252.3093	1.E-10	0.0008	5.94
7,12-Dimethylbenz[a]anthracene	57-97-6	DMBA	C20H16	256.3410		0.05	5.94
Benzo[e]pyrene	192-97-2	BeP	C20H12	252.3093		0.004	
Benzo[a]pyrene	50-32-8	BaP	C20H12	252.3093	6.E-09	0.0038	6.31
3-Methylcholanthrene	56-49-5	3MCA	C21H16	268.3517		0.0019	6.42
Indeno[1,2,3-cd]pyrene	193-39-5	Ind	C22H12	276.3307	5.E-10	0.00019	6.72
Dibenz[a,h]anthracene	53-70-3	DahA	C22H14	278.3466	1.E-09	0.0006	6.88
Benzo[g,h,i]perylene	191-24-2	BghiP	C22H12	276.3307	1.E-10	0.00026	7.04
Dibenz[a,i]pyrene	189-55-9	DbaiP	C24H14	302.3680			
Dibenz[a,h]pyrene	189-64-0	DbahP	C24H14	302.3680			
Dibenz[a,l]pyrene	191-30-0	DbalP	C24H14	302.3680			

5

Ulsan is a large industrial city located on the southeastern part of South. There are 2 massive industrial areas in east and southeast Ulsan: Mipo National Industrial Area and Onsan National Industrial Area, which together are comprised of petrochemical, non-ferrous, automobile, and shipbuilding production industries (Figure 2). Residents in Ulsan are likely to be affected by emissions of PAHs because residential areas are close to these industrial complexes. Generally, previous studies have been reported that the levels and characteristics of the PAHs in Ulsan is various seasonally depending on seasonal winds (Choi et al., 2012b; Nguyen et al., 2018). In winter and spring, winds blow towards the east sea, moving PAHs emitted from industrial areas to out of sea. Concentrations of PAHs tend to be highest in winter due to increased fossil fuel combustion for residential heating and decline of atmospheric dispersion. On the other hand, the levels of PAHs in spring are influenced more by yellow sand and long-range transport from the Northeast Asia (i.e., China and North Korea) (Thang et al., 2019). In summer, PAHs originated from industrial areas in Ulsan can move toward residential areas by southeasterly winds (Choi et al., 2012b; Clarke et al., 2014; Nguyen et al., 2018). The wind fields and wind roses during the sampling event are shown in Figure 3.

Figure 2. Industrial areas and activities in Ulsan, South Korea. The arrows show the prevailing wind direction in winter and summer.

(a) Winter
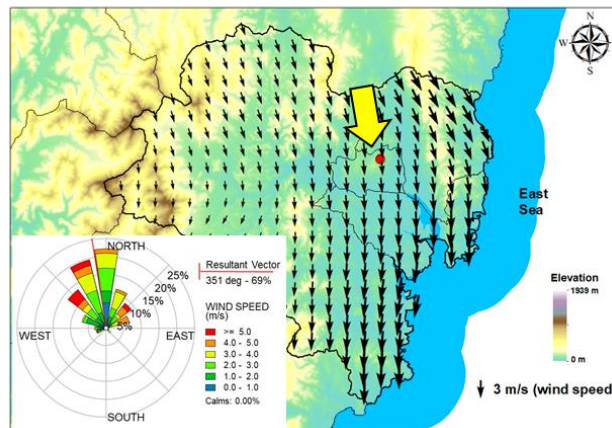
(b) Spring
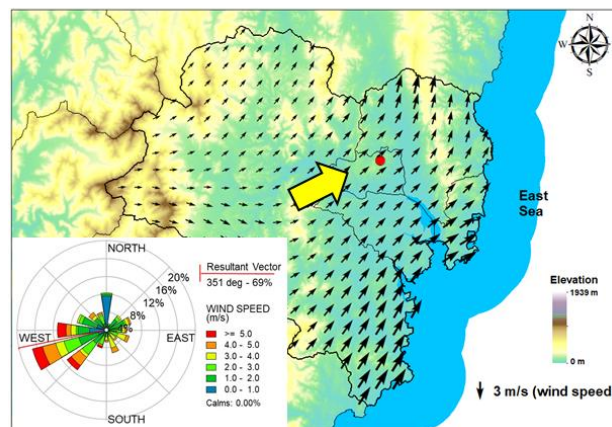
(c) Summer
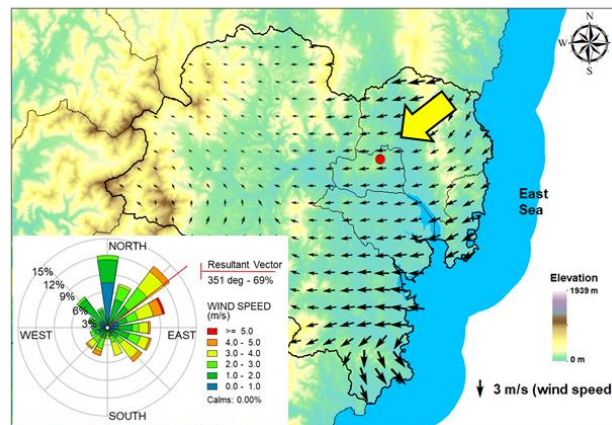
Figure 3. Wind fields and wind roses of (a) winter, (b) spring, and (c) summer in Ulsan.

The aims of this study were to investigate the seasonal concentrations, profiles and phase distribution of 21 PAHs in the atmosphere in Ulsan. In addition, the emission sources of these PAHs and the effects of long-range transport were identified seasonally. Finally, cancer risk induced by exposure of the 21 PAHs including US EPA 13 priority PAHs via inhalation was studied.

II. MATERIALS AND METHOD

2.1 Ambient air sampling

Air samples were collected at the rooftop of the Yeongnam air quality monitoring station, Ulsan, South Korea (35°34'52.36"N, 129°19'27.15"E). The Yeongnam air quality monitoring station is located at a residential area in the north and northwestern part of the urban and industrial districts in Ulsan (Figure 4). Sampling was conducted for three seasons (December 2013–August 2014). A high-volume air sampler (Sibata, HV-700F, Japan) was used to collect PAHs samples in the gaseous and particulate phases once a week. The total air volume of each sample was 1007.9 m^3 (flow rate: 700 L/min). Samples in the gaseous and particulate phase PAHs were collected using glass fiber filters (GFFs, adantec, Japan) and polyurethane foam disks (PUFs, Ziemer chromatographie, Germany), respectively.

The GFFs were baked at 400 °C for 4 h and the PUF disks were cleaned by sonication prior to sampling for 30 min with acetone and n-hexane, respectively. The cleaned GFFs and PUFs were kept in aluminum foil prior to sampling. The GFF and PUF samples after sampling were stored at -9 °C wrapped in aluminum foil and polyurethane zippered bags until analysis.

2.2 Analytical procedure

Prior to extraction, surrogate standard (naphthalene-d8 (Nap-d8), acenaphthylene-d10 (Ace-d10), phenanthrene-d10 (Phe-d10), chrysene-d12 (Chr-d12), and perylene-d12 (Per-d12)) was added to all samples and PAHs collected on GFFs and PUFs were extracted by Soxhlet extractor for 20 h with 350 mL of n-hexane/acetone (9:1). The extracts were concentrated to 10 mL using a Turvo vap (Caliper, USA) and then cleaned up on a silica gel column containing 2 g of anhydrous sodium sulfate, 5 g of activated silica gel (4 h at 130 °C), and 2 g of anhydrous sodium sulfate with 70 mL of n-hexane/dichloromethane (9:1). The effluents were concentrated to 0.5 mL using Turvo Vap and nitrogen evaporator (Eyela, Japan). These final extracts were carried to gas chromatography (GC) vial, and then an internal standard (p-terphenyl-d14) was spiked to the vial prior to instrumental analysis.

Among the target 24 PAHs, naphthalene, acenaphthylene, and acenaphthene were excluded in this study because of their low recoveries, potential sampling artifacts, and blank contamination. An Agilent 7890A gas chromatograph interface with an Agilent 5975C mass spectrometer (GC/MS, Agilent, USA) equipped with a DB-5MS capillary column (30 m × 0.25 m i.d., 0.25 μm film thickness) was used for the analysis. One μL of the final sample was injected into the GC in splitless mode at 300 °C of inlet temperature. The GC was operated under selected ion monitoring (SIM) mode and the carrier gas was helium (He) at a flowrate of 1.0 mL/min. The GC oven temperature was as follows: started at 60 °C for 1 min, increased at 10 °C/min until 320 °C, and finally held at 320 °C for 8 min.
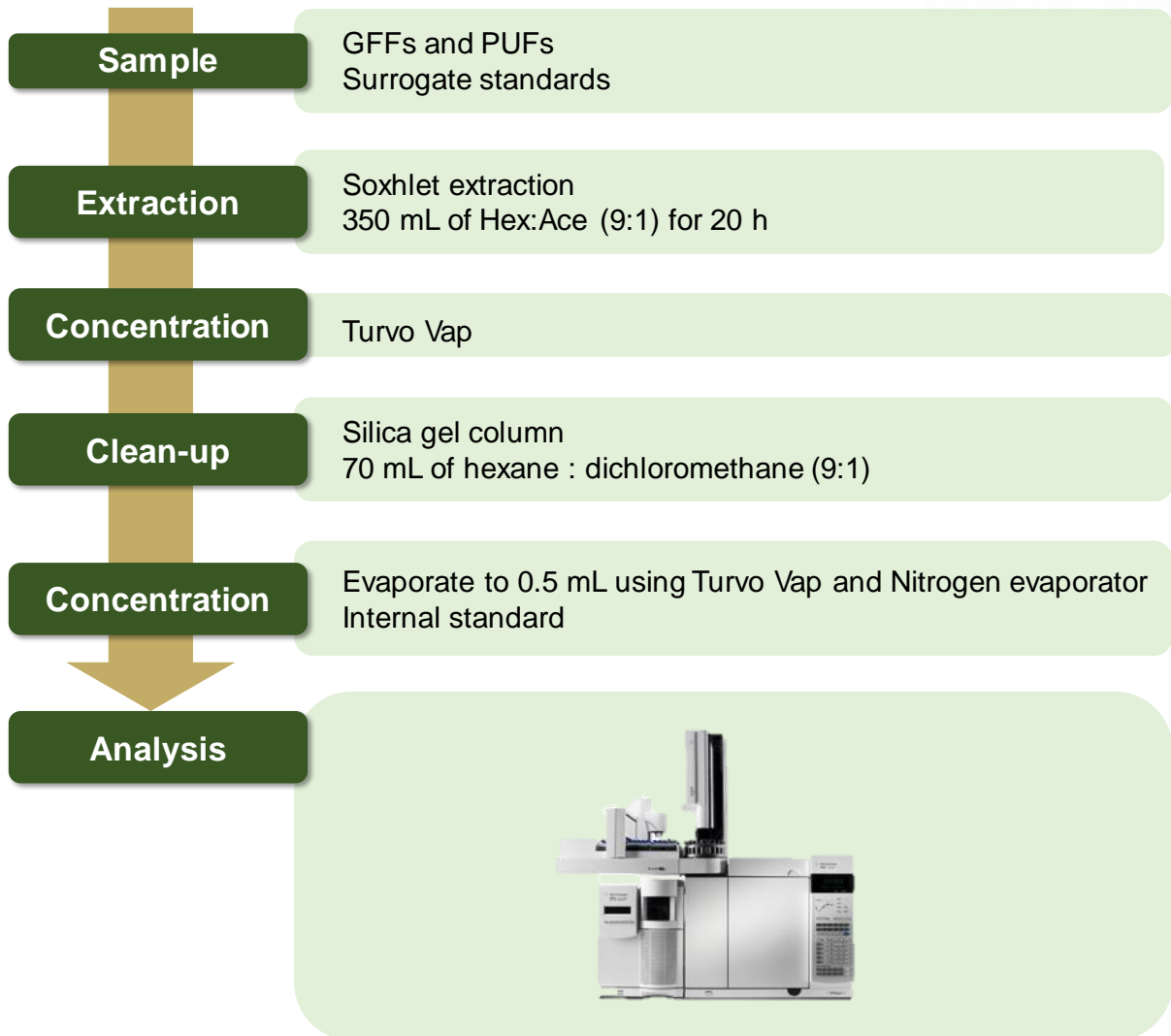
Figure 4. Analytical procedural for PAHs in GFFs and PUFs samples.

2.3 Quality assurance and quality control (QA/QC)

Field blank samples were collected to correct the contamination of sample during all processes from sampling to analysis (e.g. field, shipping to the laboratory, storage, pretreatment and analysis). The concentrations of PAHs were corrected by average blank value (n=10). Average recoveries of the PUF samples were 61%, 95%, and 85% and those of the GFF samples were 78%, 99%, and 100% for Phe-d10, Chr-d12, and Per-d12, respectively. Method detection limit (MDL) of the gaseous and particulate PAHs were calculated by the following equation:

$$MDL = SD \times 3.14 \tag{1}$$

where SD indicates the standard deviation of 7 replicates of spiked blank samples and 3.14 is the Student's t value for a 99% confidence level. Values of MDL ranged from 0.01 ng/m^3 to 0.13 ng/m^3 for PUFs and from 0.02 ng/m^3 to 0.08 ng/m^3 for GFFs. Concentrations of PAHs below the MDLs were treated as non-detects (NDs) and substituted with half of MDL values.

Table 3. MDL (ng/m^3), IDL (ng/m^3), and detection frequencies (%) of PAHs in total samples.

	MDL (ng/m^3)		IDL (ng/m^3)	Detection frequency (%)	
	PUF	GFF		PUF	GFF
Flu	0.07	0.03	0.004	94%	3%
Phe	0.08	0.05	0.001	100%	53%
Ant	0.07	0.05	0.002	63%	0%
Flt	0.10	0.07	0.019	100%	66%
Pyr	0.12	0.07	0.020	100%	69%
BcPhe	0.08	0.05	0.006	0%	25%
BaA	0.08	0.04	0.002	3%	50%
Chr	0.08	0.05	0.004	22%	69%
Bb+jF	0.09	0.03	0.003	0%	81%
BkF	0.09	0.06	0.005	0%	63%
DMBA	0.06	0.04	0.012	0%	0%
BeP	0.08	0.04	0.004	0%	78%
BaP	0.13	0.06	0.007	0%	63%
3MCA	0.08	0.04	0.022	0%	0%
Ind	0.07	0.03	0.007	0%	81%
DahA	0.07	0.06	0.008	0%	13%
BghiP	0.07	0.04	0.004	3%	75%
DbaiP	0.07	0.06	0.007	0%	0%
DbahP	0.03	0.03	0.010	0%	3%
DbalP	0.01	0.02	0.013	0%	0%

2.4 Statistical analysis

Statistical analysis has been used for analysis and interpretation of data. A Spearman correlation analysis among PAHs in ambient air, TSP, PM_{10}, and $PM_{2.5}$ was conducted to identify their respective relationships. In addition, a Shapiro-Wilk normality test and a Mann-Whitney rank sum test were conducted using SigmaPlot 12.0 (Systat Software Inc, USA). A principle component analysis (PCA) was conducted to understand pollution characteristics and estimate sources of the PAHs. The normalized PAH concentration data with only high detective frequencies (> 50%) were chosen for input data. The rotation method was varimax and eigenvalues greater than one were used for the PC extraction criterion. SPSS 20.0 software (IBM, USA) was used to perform the Spearman correlation analysis and PCA.

2.5 Backward trajectory analysis and concentration weighted trajectory (CWT)

Backward trajectory analysis, which is produced by the Hybrid Single-Particle Lagrangian Integrated Trajectory (HYSPLIT) model (https://www.ready.noaa.gov/HYSPLIT.php) has been used to analysis movement of airmass and effect of long-range transport of PAHs (Sofuoglu et al., 2013; Tang et al., 2014; Zhang et al., 2017). In this study, the backward trajectories of 72 h were calculated using the averaged data of every one hour for each 24 h sample (from 11:00 a.m. local time). The starting height of trajectories was 500 m above the ground. A total of 768 trajectories was obtained since the number of sampling day was 52 for three seasons. The input data for HYSPLIT model were listed in Table 4 and backward air trajectories during sampling period were illustrated in Figure 5.

Table 4. Input data of HYSPLIT model.

Data	Contents
Location	Yeong-Nam monitoring station
Coordinate	35°34'52.36"N, 129°19'27.15"E
Study period	Sampling date
Trajectory period	72 hours
Height	500 m above ground level
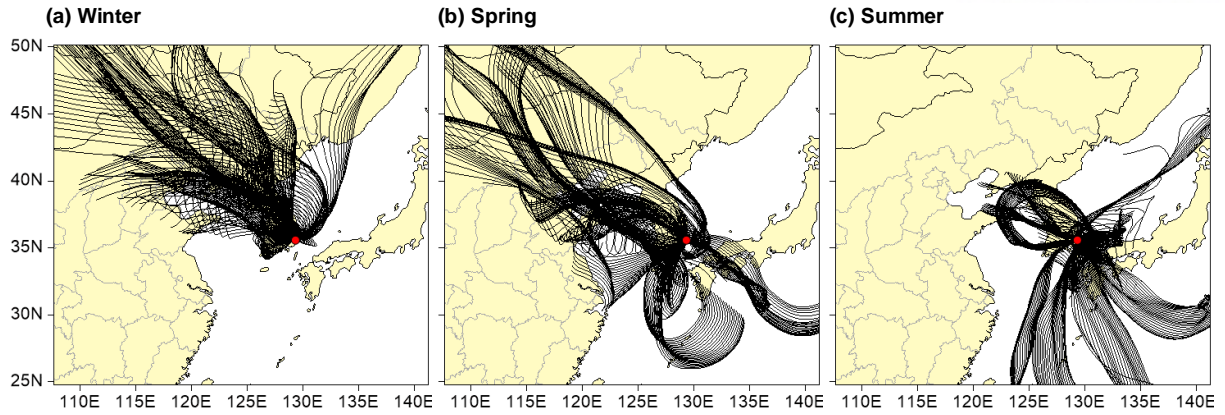
Figure 5. Backward air trajectories arriving at Ulsan, South Korea. The red point present Yeongnam air quality monitoring station.

The hybrid receptor models have been used estimate the source areas of air pollutants. Concentration weighted trajectory (CWT) assigns weighted concentration of pollutants that have associated trajectories to each cell based on the below equation:

$$CWT_{ij} = \frac{1}{\sum_{l=1}^{L} \tau_{ijl}} \sum_{l=1}^{L} C_l \tau_{ij\,l} \tag{2}$$

where CWT_{ij} denotes the CWT value of the cell i, j, C_l is the PAH concentration, L is the total backward trajectory line number, and τ_{ijl} is endpoint number of backward trajectory l in grid cell i, j (Hsu et al., 2003). TrajStat was used to calculate the CWT (Wang et al., 2009). The domain of CWT was 110°– 140°E and 25°–50°N with the grid cell of 0.5°×0.5°. The arbitrary weighted function $W(n_{ij})$ was considered to reduce the effect of the small number of trajectories passing through the i, j grid cell, n_{ij}. The weighting function $W(n_{ij})$ are expressed by Equ. (3):

$$W(n_{ij}) = \begin{cases} 1, & n \geq 2av \\ 0.75, & 2av \geq n \geq av \\ 0.5, & av \geq n \geq \frac{av}{2} \\ 0.2, & \frac{av}{2} \geq n \end{cases} \tag{3}$$

where n denotes the number of trajectory endpoints in each grid cell, and the av is the average number of trajectory endpoints per cell.

2.6 Health risk assessment

The potential cancer risk of the PAHs via inhalation were evaluated. In advance, the concentration of individual PAHs could be converted to its BaP equivalent concentration (BaP_{eq}) using below equation:

$$BaP_{eq} = C \times TEF \tag{4}$$

where BaP_{eq} is the BaP concentration of each compound (ng/m^3); C is the concentration of individual PAHs (ng/m_3); TEF is toxic equivalent factor (TEF). The TEFs of 21 PAHs were listed in Table 1.

The incremental lifetime cancer risk (ILCR) model was used to calculate the potential carcinogenicity of the PAHs via inhalation following the equation:

$$ILCR = (ISF \times BaPeq \times IR \times EF \times ED \times cf) / (BW \times AT) \tag{5}$$

where ISF (mg/kg/day) is inhalation slope factor, IR (m^3/h) is inhalation rate, EF (day/year) and EP (year) denote the exposure frequency and exposure duration, respectively. cf (10^{-6}) is the conversion factor. BW (kg) and AT (days) represent the body weight and averaging time, respectively. The cancer risk of Σ_{21} PAHs and Σ_{13} PAHs were calculated to estimate increase of cancer risk for Σ_{21} PAHs than those for Σ_{13} PAHs. However, high uncertainty was expected for the values in Equ. (5). Therefore, Monte Carlo simulation was used to decrease the uncertainty of estimations using Crystal Ball 11.1 (Oracle, USA) with 10,000 iteration. The risk parameters used in this study are shown in Table 5.

Table 5. Input data of Monte Carlo simulation to estimate cancer risk through inhalation.

Variable	Name	Unit	Value			Data distribution			Reference
			Winter	Spring	Summer	Winter	Spring	Summer	
BaP_{eq_13}	BaP_{eq} (Σ_{13} PAHs)	ng/m^3	A (0.48, 0.35)	A (0.22, 0.13)	A (0.11, 0.04)	normal	normal	normal	this study
BaP_{eq_21}	BaP_{eq} (Σ_{21} PAHs)	ng/m^3	A (0.61, 0.44)	A (0.27, 0.15)	A (0.17, 0.12)	normal	log-normal	log-normal	this study
BW	Body weight	kg		G (62.8, 10.9)			log-normal		MOE (2007); NIER (2016a)
EF	Exposure factor	day/year		G (252, 1.01)			log-normal		Chen and Liao (2006)
ED	Exposure duration	year		U (0, 52)			uniform		this study
AT	Averaging time	day		22,550			constant		Nguyen et al. (2020)
IR	Inhalation rate	m^3/h		A (14.3, 1.1)			log-normal		MOE (2007); NIER (2016a)
ISF	Inhalation slope factor for BaP	mg/kg/day		3.9			constant		CalEPA (2009)

A (m, sd): Arithmetic mean and standard deviation

G (gm, gsd): Geometric mean and standard deviation

U (min, max): Minimum and maximum data

III. RESULTS AND DISCUSSION

3.1 Monitoring of 21 PAHs

3.1.1 Levels and trends of PAHs

The range and mean concentrations of PAHs in gaseous, particulate, and total (gaseous + particulate) phases over the sampling period are listed in Table 6. The total concentrations of PAHs were in the range of 1.46–17.56 (mean: 7.40) ng/m^3 for the gaseous, 0.28–12.78 (mean: 2.72) ng/m^3 for the particulate, and 1.84–29.72 (mean: 10.11) ng/m^3 for the total phases, respectively. The 3-ring PAHs (Flu, Phe, and Ant) were detected in all PUF samples, but only 34% of Flu, 84% of Phe, and 62% of Ant were detected in the GFF samples. The 4-ring PAHs, except for DMBA, were highly detected in both PUF and GFF samples. The 5- and 6-ring PAHs, except for 3MCA, were frequently detected in the GFF rather than the PUF samples. DMBA and 3MCA, which are known not to be originated from environment source (Collins et al., 1998), were absent in all samples.

Table 6. Range and mean concentrations (ng/m3) of the gaseous, particulate, and total (gas + particle) PAHs for entire sampling period in Ulsan.

Ring No.	Compounds	Gas		Particle		Total	
		Range	mean	Range	mean	Range	mean
3	Flu	ND–6.69	1.30	ND–0.04	0.01	0.01–6.71	1.30
3	Phe	0.37–7.69	3.69	ND–0.79	0.10	0.39–8.10	3.79
3	Ant	ND–0.75	0.16	ND–0.03	0.02	0.01–0.78	0.17
4	Flt	0.37–2.25	1.17	ND–2.28	0.40	0.45–4.04	1.57
4	Pyr	0.21–2.54	0.97	ND–1.77	0.32	0.38–2.76	1.29
4	BcPhe	-	0.01	ND–0.28	0.06	0.04–0.29	0.07
4	BaA	N.D.–0.11	0.01	ND–0.60	0.10	0.01–0.61	0.11
4	Chr	N.D.–0.19	0.03	ND–1.22	0.23	0.04–1.23	0.26
5	Bb+jF	-	0.01	ND–1.50	0.32	0.02–1.50	0.32
5	BkF	-	0.01	ND–0.72	0.16	0.03–0.73	0.17
4	DMBA	-	ND	-	ND	-	ND
5	BeP	-	0.01	ND–1.18	0.28	0.02–1.19	0.29
5	BaP	-	0.01	ND–0.56	0.13	0.03–0.58	0.14
5	3MCA	-	ND	-	ND	-	ND
6	Ind	-	0.01	ND–1.20	0.27	0.02–1.21	0.28
5	DahA	-	0.00	ND–0.10	0.03	ND–0.10	0.03
6	BghiP	ND–0.22	0.01	ND–1.01	0.27	0.03–1.02	0.28
6	DbaiP	-	ND	-	ND	-	ND
6	DbahP	-	0.00	ND–0.03	0.00	ND–0.03	0.00
6	DbalP	-	ND	-	ND	-	ND
	Σ_{21} PAHs	1.46–17.56	7.40	0.28–12.78	2.72	1.84–29.72	10.11

Figure 6 shows the PAH concentrations in three seasons. The mean Σ_{21} PAH concentrations were highest in winter (mean: 13.06 ng/m^3), followed by spring (7.67 ng/m^3) and summer (6.03 ng/m^3). The results of t-test and rank-sum test demonstrated the difference between winter and other seasons ($p = 0.012$ between winter and spring, $p < 0.001$ between winter and summer). This pattern is in accordance with previous studies (Ichikawa et al., 2018; NIER, 2016b; 2018; 2019). This seasonal trend was shared for the gaseous (winter: 7.48 ng/m^3, spring: 5.57 ng/m^3, and summer: 5.35 ng/m^3) and particulate (winter: 5.57 ng/m^3, spring: 2.21 ng/m^3, and summer: 0.68 ng/m^3) PAHs. Generally, increased fuel combustion for heating and less dispersion in the atmosphere due to low temperature and low mixing height lead to the elevated levels of PAHs in winter. On the other hand, in summer, high atmospheric temperature and solar radiation induce photodegradations between PAHs and atmospheric oxidants (Baek et al., 1991). Moreover, an increase of the mixing layer and a lack of major PAHs sources or residential combustions for heating could explain for the lowest level of PAHs in summer (Nguyen et al., 2018).
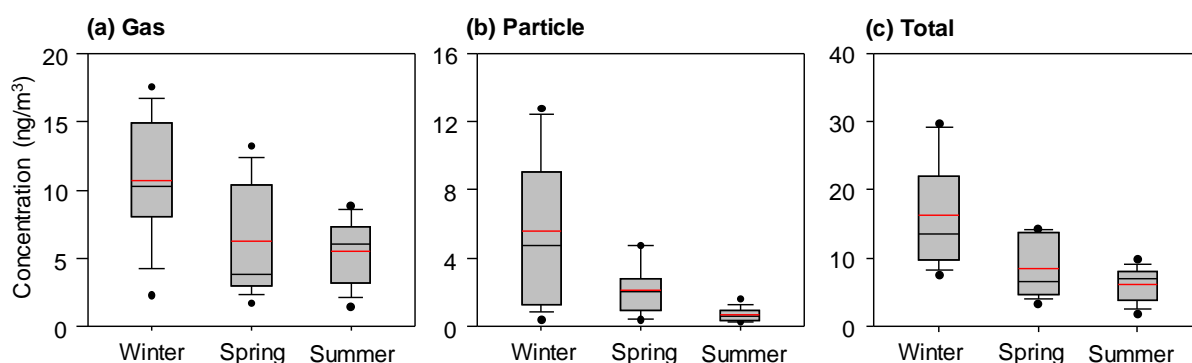
Figure 6. Seasonal concentrations of the total Σ_{21} PAHs in (a) the gaseous, (b) particulate, and (c) total (gaseous + particulate) phases.

The sum of 8 PAHs (BcPhe, BjF, DMBA, BeP, 3MCA, DbaiP, DbahP, and DbalP) in the total (gaseous + particulate) phase ranged from 0.07 to 2.23 ng/m^3 (mean: 0.53 ng/m^3) and contributed highest in winter (6.3%), followed by spring (5.2%) and summer (2.6%) (Figure 7). In addition, the particulate fraction (19.0%) of the Σ_8 PAHs was more dominant compared to the gaseous one (0.3%). These Σ_8 PAHs, consisting of middle- and high-molecular weight PAHs, tends to be partitioned in the particulate phase. Additionally, similar seasonal trends between the Σ_8 PAHs and the US EPA priority Σ_{13} PAHs indicate that the Σ_8 PAHs might be influenced by similar emission sources to the Σ_{13} PAHs.

The Σ_{21} PAH concentrations in residential areas of several countries were compared with those in this study and shown in Table 7. Only a few studies have investigated the concentrations of 21 PAHs in the ambient air. The concentration of particulate Σ_{21} PAHs (2.70 ng/m^3) observed in this study were lower

than those found in other sites in South Korea (Yeongam-Gun: 22.3 ng/m^3, Gwangju: 3.93 ng/m^3, Daejeon: 6.21 ng/m^3) and similar to those in Japan (2.86 ng/m^3). The PAH concentrations in the both particulate and gaseous phases were higher than those in Sweden (6.44 ng/m^3) and Canada (6.57 ng/m^3), and lower than those in Uganda (27.7 ng/m^3). The proportion of Σ_8 PAHs among Σ_{21} PAHs (18.6%) in the particulate phase were lower than those of the other residential sites in South Korea (Yeongam-Gun: 23.4%, Gwangju: 25.0%, Daejeon: 28.3%), and comparable to those in Japan (19.9%) and Sweden (17.7%).
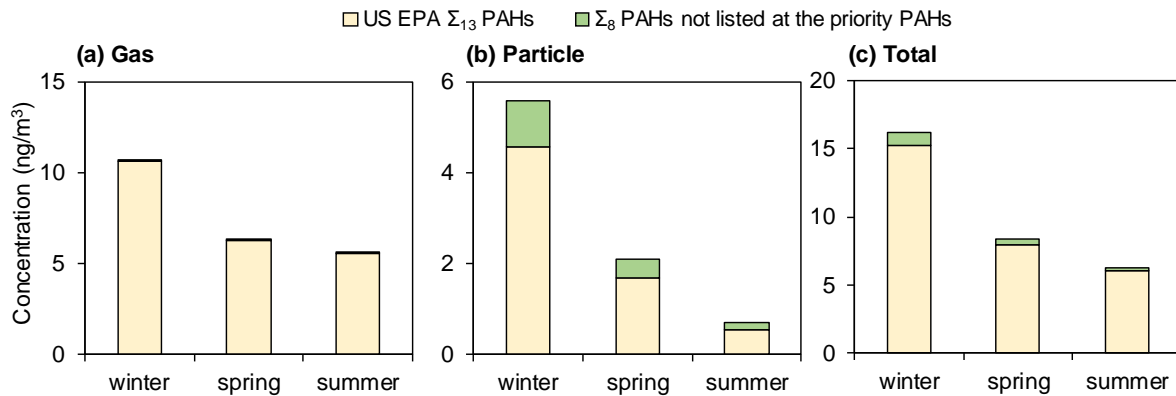
Figure 7. Concentrations of US EPA Σ_{13} PAHs and other Σ_8 PAHs not listed at the priority PAHs in (a) the gaseous, (b) particulate, and (c) total (gas + particle) phases.

Table 7. Comparison of total $\Sigma 21$ PAHs, US EPA $\Sigma 13$ PAHs, other $\Sigma 8$ PAHs, and ratio of $\Sigma 13$ PAHs/ $\Sigma 8$ PAHs between this study and previous studies.

Country	Location	Sampling period	Sample type	Σ_{21} PAH	Σ_{13} PAH[a]	Σ_8 PAH[b]	Σ_8 PAH/Σ_{21} PAH	Reference
Japan	Chiba	Jun 2016–Oct 2017	PM$_{2.5}$	2.86	2.29	0.57	19.9%	Ichikawa et al. (2018)
Canada	Alberta	Jan 2012–Dec 2013	TSP and PUF	6.57	6.13	0.44	6.70%	Hsu et al. (2015)
Uganda	Entebbe	Oct 2008–Jul 2010	TSP and PUF	27.7	26.8	0.94	3.39%	Arinaitwe et al. (2012)
Sweden*	Stockholm	Oct 2012–Dec 2013	PUF	5.47	5.44	0.02	0.45%	Masala et al. (2016)
Sweden*	Stockholm	Oct 2012–Dec 2013	TSP	0.97	0.80	0.17	17.7%	Masala et al. (2016)
South Korea	Yeongam-Gun	Aug 2015–May 2016	TSP	22.3	1.79	0.55	23.4%	NIER (2016b)
South Korea	Gwangju	Jan 2018–Sep 2018	TSP	3.93	2.85	0.98	25.0%	NIER (2018)
South Korea	Daejeon	Oct 2018–Jun 2019	TSP	6.21	4.45	1.76	28.3%	NIER (2019)
South Korea	Ulsan	Nov 2013 - Aug 2014	TSP	2.70	2.20	0.50	18.6%	This study
South Korea	Ulsan	Nov 2013 - Aug 2014	PUF	7.39	7.37	0.02	0.30%	This study
South Korea	Ulsan	Nov 2013 - Aug 2014	TSP and PUF	10.1	9.57	0.53	5.21%	This study

* 21 PAHs except for DMBA and 3MCA

[a] 16 US EPA PAHs except for Nap, Acy, and Ace

[b] BcPhe, BjF, DMBA, BeP, 3MCA, DbaiP, DbahP, and DbalP

The PAHs showing the detected frequencies greater than 50 % were used to analyze their correlation to particulate matter (i.e., TSP, PM_{10}, and $PM_{2.5}$). The results of Spearman correlation analysis among each PAH compound and Σ_{21} PAHs in gaseous phase and particulate phase, TSP, PM_{10}, and $PM_{2.5}$ were shown in Table 8 and 9, respectively. PM_{10} and $PM_{2.5}$ concentrations were measured at Yeongnam air quality monitoring station (35°34'52.36"N, 129°19'27.15"E) using beta ray attenuation method (BAM 1020, USA). The sum of Σ_{21} PAHs in gaseous phase showed strong correlation with each compounds except for Chr, suggesting the behavior of gaseous PAHs is governed by 3-ring PAHs and some of 4-ring PAHs (Flt and Pyr), having relatively low-molecular-weight (< 203). The particulate PAHs has strong correlation with Σ_{21} PAHs as well as each other, suggesting the common pollution sources of PAHs. Moreover, the particulate Σ_{21} PAHs had positive correlation with TSP, PM_{10}, and $PM_{2.5}$. Among particulate matters, the particulate Σ_{21} PAHs showed the strongest correlation with TSP, followed by PM_{10}, and $PM_{2.5}$. Since the Σ_{21} PAHs contains all PAH species from 3- to 6-ring, the particulate Σ_{21} PAHs showed the strongest correlation with TSP.

Table 8. Spearman correlations among gaseous PAHs, TSP, PM10, and PM2.5 during three sampling seasons.

	Flu	Phe	Ant	Flt	Pyr	Chr	ΣPAHs	TSP	PM$_{10}$	PM$_{2.5}$
Flu	1.000	.759**	.645**	.554**	.200	.031	.802**	-.023	.101	.105
Phe		1.000	.775**	.868**	.703**	.361*	.974**	.020	.086	.086
Ant			1.000	.828**	.654**	.359*	.842**	-.008	-.097	.010
Flt				1.000	.879**	.511**	.899**	.105	.130	.170
Pyr					1.000	.567**	.691**	.006	-.018	.080
Chr						1.000	.337	.294	.278	.286
ΣPAHs							1.000	.017	.062	.097

*Correlation is significant at the 0.05 level.

**Correlation is significant at the 0.01 level.

23

Table 9. Spearman correlations among particulate PAHs, TSP, PM_{10}, and $PM_{2.5}$ during three sampling seasons.

	Phe	Flt	Pyr	BaA	Chr	BbjF	BkF	BeP	BaP	Ind	DahA	BghiP	ΣPAHs	TSP	PM_{10}	$PM_{2.5}$
Phe	1.000	.583**	.602**	.561**	.575**	.562**	.510**	.496**	.671**	.544**	.624**	.538**	.669**	.442*	0.334	0.348
Flt		1.000	.986**	.861**	.974**	.906**	.907**	.917**	.876**	.920**	.603**	.916**	.922**	.414*	.429*	.438*
Pyr			1.000	.890**	.984**	.932**	.895**	.921**	.888**	.937**	.610**	.921**	.952**	.452**	.431*	.414*
BaA				1.000	.905**	.886**	.850**	.836**	.877**	.891**	.608**	.851**	.916**	0.273	0.295	0.273
Chr					1.000	.938**	.909**	.937**	.900**	.941**	.623**	.927**	.951**	.445*	.446*	.444*
BbjF						1.000	.946**	.965**	.932**	.987**	.626**	.967**	.972**	.527**	.491**	.444*
BkF							1.000	.966**	.910**	.953**	.623**	.973**	.920**	.418*	.457*	.444*
BeP								1.000	.898**	.967**	.607**	.988**	.938**	.483**	.481**	.457*
BaP									1.000	.930**	.668**	.920**	.931**	.506**	.506**	.496**
Ind										1.000	.646**	.980**	.963**	.475**	.494**	.458*
DahA											1.000	.622**	.671**	0.276	.375*	.495*
BghiP												1.000	.948**	.483**	.510**	.470*
ΣPAHs													1.000	.497**	.461*	.419*

*Correlation is significant at the 0.05 level.

**Correlation is significant at the 0.01 level.

3.1.2 Phase distributions and profiles

The annual mean gaseous and particulate Σ_{21} PAHs concentrations were 7.39 ng/m^3 and 2.70 ng/m^3, respectively. The mean gaseous Σ_{21} PAHs concentration was approximately 2.7 times higher than the particulate one (Mann-Whitney rank sum test, $p \leq 0.001$). In general, the high mobility of gaseous PAHs could lead the shorter half-life of gaseous PAHs than the particulate ones (Ravindra et al., 2008). Moreover, photochemical degradation during transport of gaseous PAHs in the atmosphere causes their decrease levels at the receptors (Choi et al., 2012a). Therefore, the high concentrations of gaseous PAHs in this study can be explained by the effects of local emission sources. The contribution of particulate PAHs was greatest in winter (34.3%), followed by spring (25.1%) and summer (11.1%) (Figure 8). Added to this, the proportion of particulate PAHs in winter and spring were statistically different from those in summer (Mann-Whitney rank-sum test, $p < 0.05$). This is probably due to as increase of PAH emissions as well as TSP concentrations in winter (mean: 99.8 µg/m^3) and spring (mean: 145.7 µg/m^3) than those in summer (mean: 79.9 µg/m^3) from residential heating or long-range transport during winter and spring. Moreover, the high temperature and sunlight intensity in summer change the gas/particle distribution of PAHs, resulting in a shift of particulate PAHs towards the gaseous phase (Esen et al., 2008; Kiss et al., 1998).
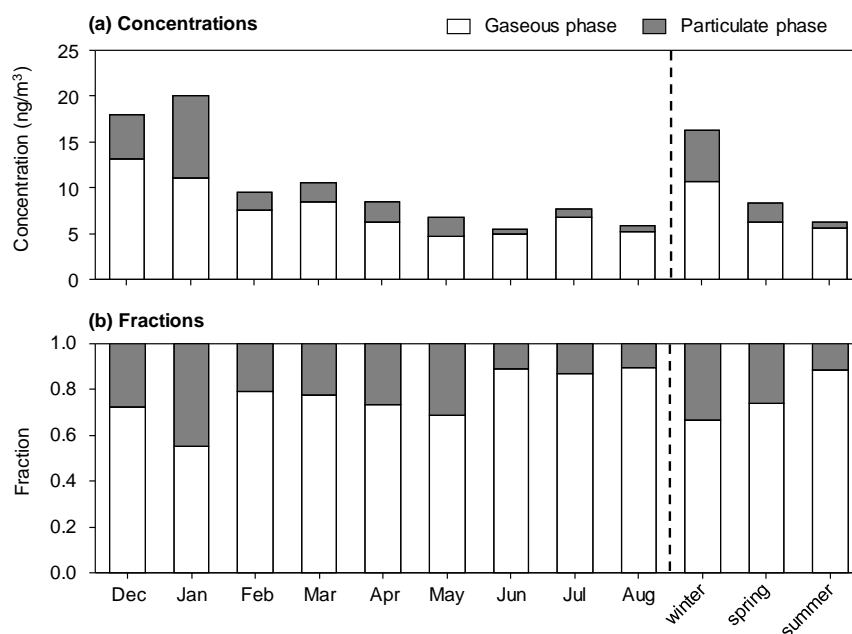
Figure 8. (a) The concentrations and (b) phase distributions of Σ_{21} PAHs shown in monthly and seasonal variations.

25

Figure 9 illustrates the profiles of Σ_{21} PAHs in the gaseous, particulate, and total phases. The concentrations of PAH species in the gaseous, particulate, and total phase are shown in Figure 10. For the gaseous phase, the 3-ring (69.5%) and 4-ring (29.7%) PAHs were predominant, in particular, the fractions of 3-ring PAHs increased in winter compared to those in summer (winter: 21.8%, spring: 33.2%, winter: 39.6%). For the particulate phase, the concentration of PAHs decreased dramatically but this trend was not observed for the ring fractions. The 4-ring PAHs were most abundant (41.7%), followed by the 5-, 6-, and 3-ring PAHs (33.3%, 20.3%, and 4.6%, respectively). Notably, the 5- and 6-ring PAHs were obviously contributed in the particulate phase due to the sorption of PAHs to particle matters. This result is consistent with previous studies (Choi et al., 2012a; Nguyen et al., 2018).
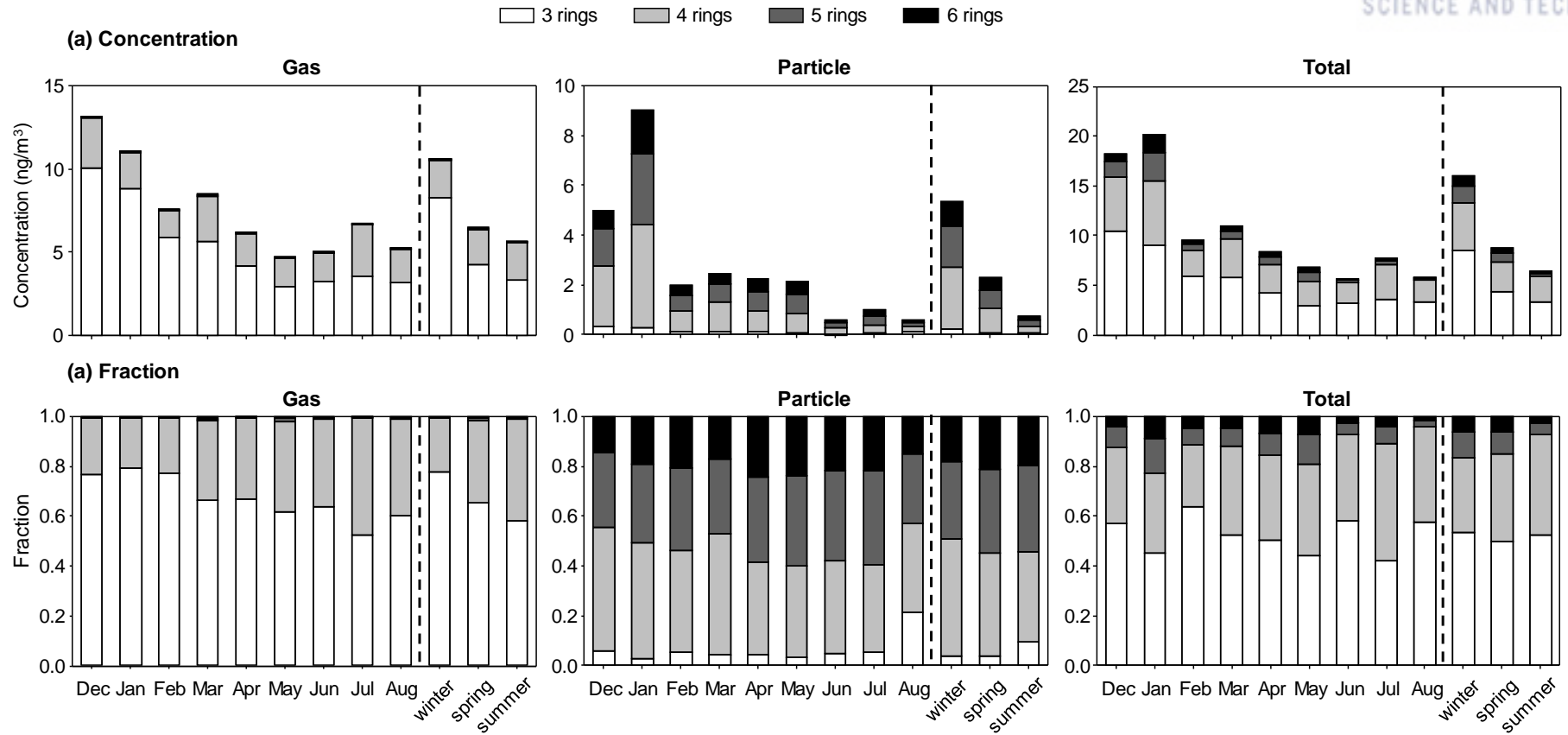
Figure 9. Monthly and seasonal variations of the PAHs shown in ring number groups: (a) concentrations and (b) fractions in the gaseous, particulate, and total phases.
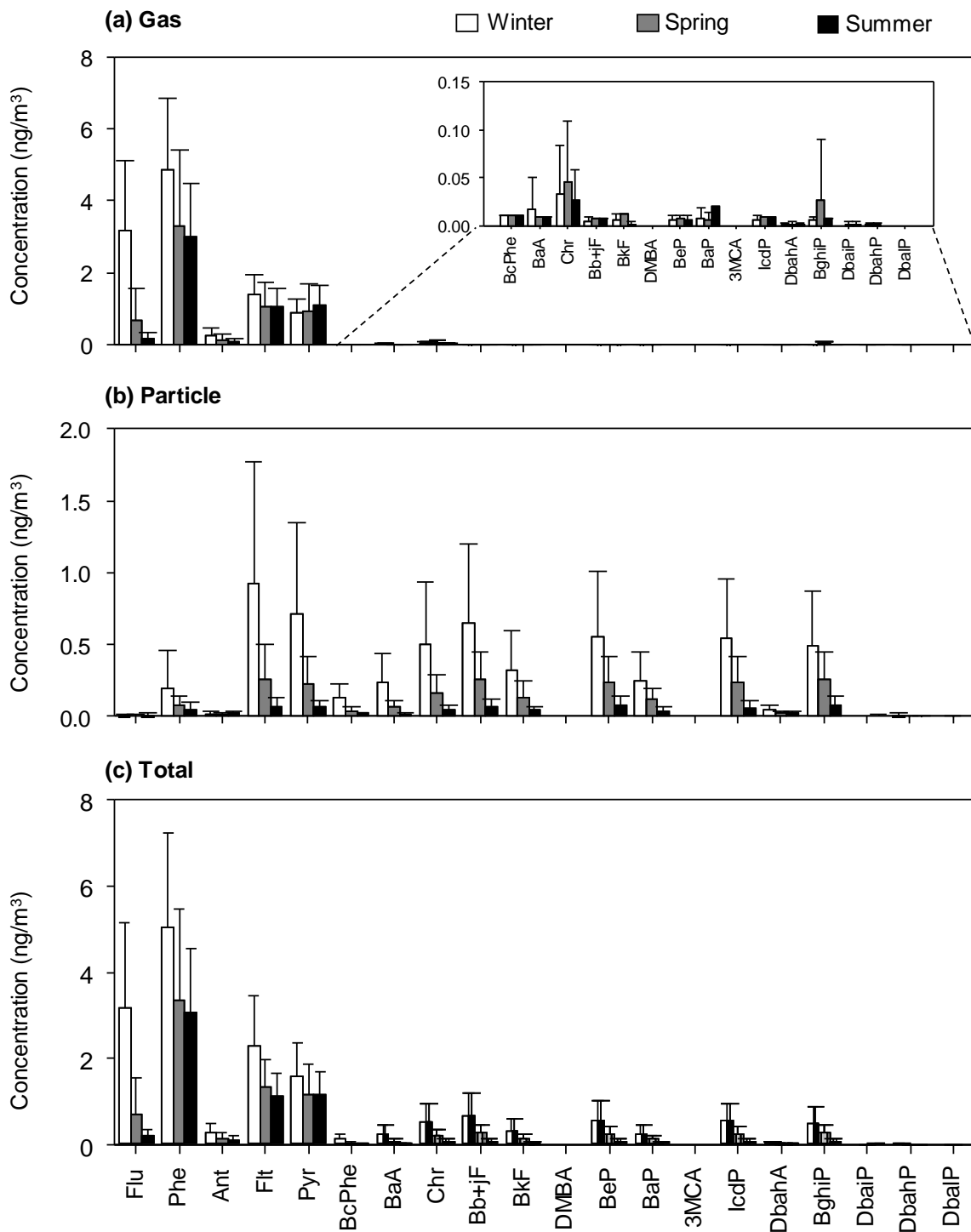
Figure 10. Concentrations of each PAH species in (a) the gaseous, (b) particulate, and (c) total (gaseous + particulate) phases in three sampling seasons.

3.2 Source identification of 21 PAHs

3.2.1 Source identification

The PCA results for gaseous and particulate PAHs in three seasons are shown in Figure 11. In order to avoid detection limit artifacts (Choi et al., 2012b), the compounds over 50% of detection frequency (gaseous PAHs: Flu, Phe, Ant, Flt, Pyr, and Chr, particulate PAHs: Phe, Ant, Flt, Pyr, BcPhe, BaA, Chr, Bb+jF, BkF, BeP, BaP, IchP, DahA, and BghiP) were used as input data.

As a result, the gaseous PAHs in spring and summer were not separated, suggesting that they might be affected by similar emission sources. These PAHs located at right side of the score plot (Figure 11a), and characterized by Phe, Flt, Pyr, and IchP. Previous studies reported that Phe, Flt, and Pyr are good markers for incineration source (de Andrade et al., 2010). Additionally, Flt and Ind are related to combustion of lubricating oil (Daisey et al., 1986). The samples in winter were well separated from other seasons, and had strong loadings of Flu and Ant which could be originated from wood combustion (Fang et al., 2004).

The particulate PAHs in winter were located at the left and upper sides, characterized by Flt, Pyr, BcPhe, BaA, Chr, and BaP (Figure 11c). BaA and BaP are typical tracers for gasoline and diesel emission (de Andrade et al., 2010; Harkov and Greenberg, 1985), while BaA and Chr have been attributed to natural gas combustion (Rogge et al., 1993; Simcik et al., 1999). Flt and Pyr are makers for the grass burning (Simoneit, 2002). Especially, BcPhe is positioned beside BaP, suggesting BcPhe might be generated by same sources of BaP. The particulate PAHs in spring were located right and bottom side, characterized by Bb+jF, BeP, Ind, and BghiP. BeP and BbF are generated from natural-gas home burning (Rogge et al., 1993), Ind and BghiP are related to automotive vehicle emission (de Andrade et al., 2010; Kulkarni and Venkataraman, 2000). Notably, some of the samples were overlapped with the winter samples, denoting that PAHs in these seasons were influenced by same emission sources. On the other hand, all the summer samplers were spread out, reflecting that various sources (e.g., petrochemical, non-ferrous metal, and heavy industries) could affect PAHs at the receptor site (Choi et al., 2012b; Nguyen et al., 2018). Briefly, PAHs in winter were associated with vehicle emission and residential heating and those in spring and summer were influenced by traffic emission and industrial activities.
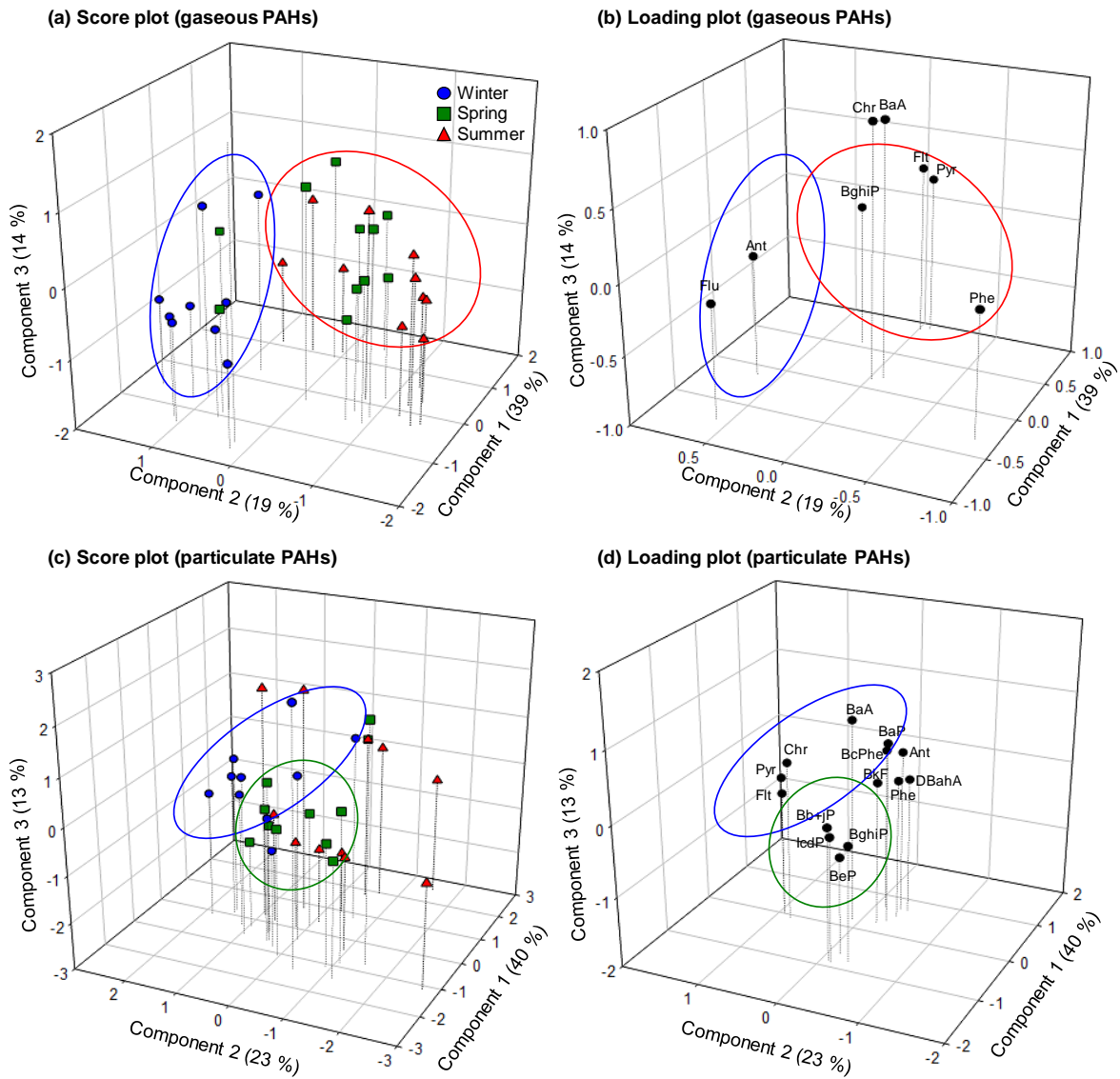
Figure 11. 3-D scatter plot of PCA results: (a) score and (b) loading plots for gaseous PAHs and (c) score and (d) loading plots for particulate PAHs.

Figure 12 presents diagnostic ratios of gaseous and particulate PAHs during three seasons. Flt/(Flt+Pyr) ratio is frequently used to separate petrogenic and pyrogenic sources (Yunker et al., 2002). PAHs originated from petrogenic sources are characterized by the ratio less than 0.5, on the other hand, those originated form pyrogenic sources are characterized by the ratio more than 0.5. A ratio of Flu/(Flu+Pyr) > 0.5 accounts for coal and biomass combustion, while the ratio between 0.4 and 0.5 accounts for petroleum combustion and the ratio less than 0.4 indicates petroleum sources. As shown in Figure 12a, the gaseous PAHs in summer might be emitted from petrogenic source, whereas those in winter were obviously originated from pyrogenic sources.

The ratio of Ind/(Ind+BghiP) could discriminate petroleum combustion from coal and biomass burning (Yunker et al., 2002). The BaA/(BaA+Chr) ratio could distinguish petrogenic (< 0.2), coal combustion (0.2–0.35), and vehicular emissions (> 0.35) (Akyuz and Cabuk, 2010; Yunker et al., 2002). These two ratios suggested that pyrogenic sources (e.g., coal/biomass burning) were dominant in winter and various pyrogenic sources including petroleum, coal and biomass combustion were dominant in spring. Furthermore, both pyrogenic and petrogenic sources were identified in summer. Therefore, both gaseous and particulate PAHs in summer were emitted from petrogenic sources and transported by southeasterly wind passing through industrial complexes (Figure 3). In addition, those in winter were obviously originated from pyrogenic sources, especially coal and biomass burning for residential heating.
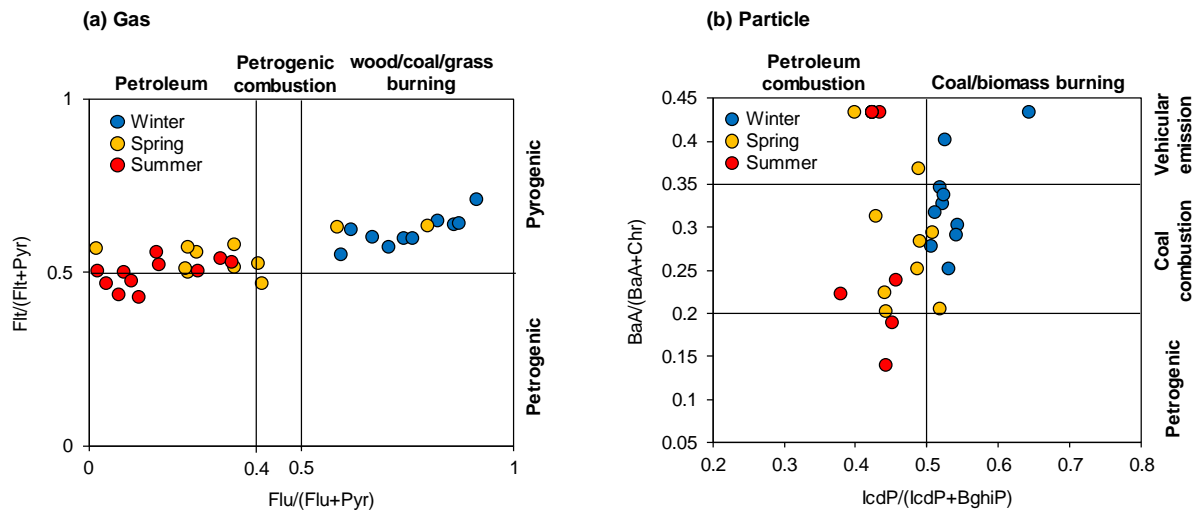
Figure 12. Diagnostic ratios of PAHs in (a) the gaseous and (b) particulate phases: (a) Flu/(Flu + Pyr) versus Flt/(Flt + Pyr) and (b) Ind/(Ind + BghiP) versus BaA/(BaA + Chr).

Since atmospheric BaP decomposes faster than BeP by photochemical reaction, the BeP/BaP ratio indexes the aging of PAHs (Lee et al., 2011; Thang et al., 2019). This ratio can also suggest the emission sources; for instance, 1.1–13 for gasoline vehicle, 2–2.5 for diesel exhaust, 0.84–1.6 for coal combustion, and 0.44 for biomass burning (Simcik et al., 1999). Previous studies mentioned that BeP/BaP should be considered carefully because the diversity of combustion sources and the effects of aging could influence the ratio (Lee et al., 2006).

The trend of BeP/BaP ratios in the particulate phase is presented in Figure 13. The ranges of the ratio in winter, spring, and summer respectively were 0.75–6.19 (mean: 2.23±1.53), 0.71–3.98 (mean: 2.10±1.04), and 0.75–3.62 (mean: 1.79±1.13). As shown in Table 10, the BeP/BaP ratios in Ulsan in winter were similar with those in Gwangju and Daejeon, South Korea and Guangzhou, China, whereas the values in this study were higher than those in Seoul, Gosan, Daesan, and Yeongam-Gun, South Korea, Shinzuoka, Japan, Xian and Beijing, China, and Mumbai, India. The air parcel could pass China and North Korea prior to arriving in Ulsan (Figure 5), suggesting that PAH in Ulsan could be affected by long-range transport. Therefore, the high BeP/BaP values in winter could indicate the increase of long-range transport effect. In spring, the BeP/BaP ratio in Ulsan were higher than the other regions in South Korea except for Gwangju, suggesting that longer residence time of air parcels (Figure 5) could increase the ratio of BeP/BaP in Ulsan. Especially, the air trajectories in the two samples with high BeP/BaP ratio passed the northeastern and eastern China, supporting the long-range transport effect in winter and spring.

In summer, the endpoints of backward air trajectories were located above the Yellow Sea, East Sea, North Korea, and South Korea, indicating PAHs in Ulsan might be affected more by local emission sources than long-range transport (Figure 5). In addition, high temperature and solar radiation could reduce the residence time of atmospheric PAHs, supporting the local source effect. The BeP/BaP ratios in summer were mostly in range of gasoline and diesel emissions, suggesting that vehicle emission were PAH sources. The BeP/BaP values in Ulan were similar to those in Seoul. Previous studies reported that these values in Seoul could suggest the effect of vehicular emissions in summer (Lee et al., 2011; Lee et al., 2008). Shortly, the BeP/BaP ratio in Ulsan could suggest that PAHs in winter and spring could be affected by long-range transport, whereas those in summer were mostly contributed by the local emissions (i.e., vehicle emission).
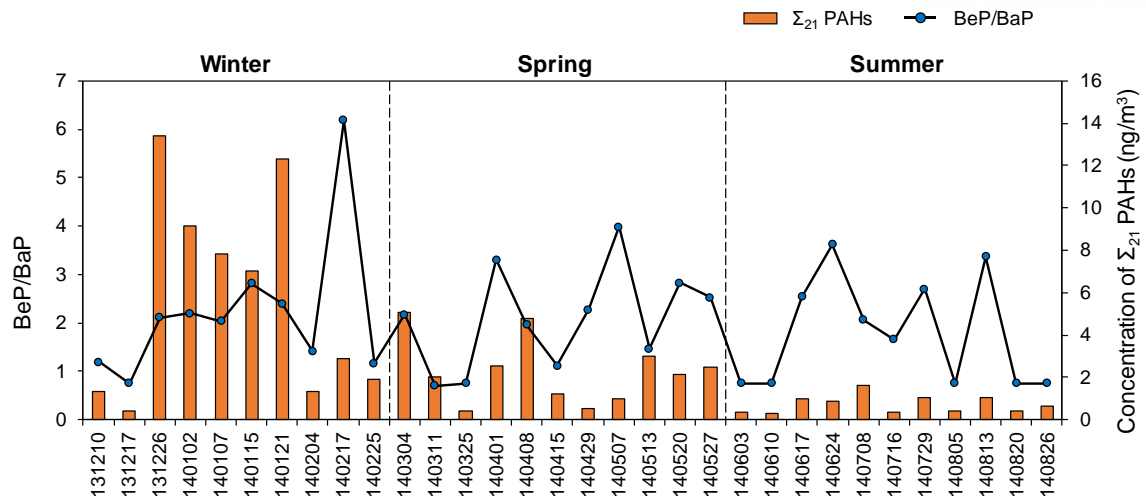
Figure 13. Temporal variations of BeP/BaP ratios and Σ_{21} PAHs concentrations during the sampling period.

Table 10. Comparison of BeP/BaP ratios from selected Asian countries.

Country	Location	Site type	Winter	Spring	Summer	Reference
South Korea	Ulsan	residential	2.2±1.5 (0.7–6.2)	2.1±1.0 (0.7–4.0)	1.8±1.1 (0.7–3.6)	this study
South Korea	Seoul	urban	(0.5–0.6)	(0.5–1.1)	(0.5–1.5)	Lee et al. (2011)
South Korea	Seoul	urban	(0.4–1.5)		(1.0–3.0)	Lee et al. (2008)
South Korea	Gosan	background	(0.3–2.4)	(0.1–2.3)	(0.0–1.7)	Lee et al. (2006)
South Korea	Daesan	industrial	(1.0–1.3)	(1.2–1.4)	(1.5–1.6)	Thang et al. (2019)
South Korea	Yeongam-Gun	residential	0.6	0.8	1.2	NIER (2016b)
South Korea	Gwangju	residential	2.8	2.9	1.2	NIER (2018)
South Korea	Daejeon	residential	2.6	1.2	0.8	NIER (2019)
Japan	Shinzuoka	urban	1.5	1.0	1.1	Kume et al. (2007)
China	Xian	urban	1.4±0.4		2.3±0.4	Ren et al. (2017)
China	Guangzhou	urban	2.0±0.2		2.9±1.2	Ren et al. (2017)
China	Beijing	urban	1.1	2.4	2.9	Huang et al. (2006)
India	Mumbai	urban	1.2			Masih et al. (2019)

mean ± std (range)

3.2.2 Long-range transport effect

Figures 14, 15, and 16 illustrate CWT of Σ_{21} PAHs and BaP in gaseous and particulate phases arriving in Ulsan over the three sampling seasons. Low-molecular weight PAHs (i.e., Phe, Flt, and Pyr), which are have a short half-life time (55–170 h) (Mackay et al., 2006b), are dominant in gaseous PAHs. The gaseous PAHs emitted from northern and northeastern China may arrive in Ulsan because the air from northern and northeastern China could arrive in Ulsan within 72 h (Kim et al., 2016a). However, the half-life time of BaP in the gaseous phase is just a few hours (Cohen and Clay, 1994). Therefore, the gaseous BaP could be mostly affected by local sources.

In winter, CWT highlighted different regions between gaseous and particulate phases (Figure 14). Northern and northeastern China (i.e., Heilongjiang, Jilin, Liaoning, and Inner Mongolia) could contribute more to the gaseous PAHs in Ulsan. Also, CWT revealed that the particulate Σ_{21} PAHs including BaP could be affected by emission sources in northeastern China (i.e., Heilongjiang, Jilin, Liaoning and Inner Mongolia), North Korea, and South Korea. In addition, prevailing northwesterly surface winds in winter suggest that local emissions from industrial areas in the southern and southeastern areas of Ulsan could be transported toward East Sea (Figure 3a). Therefore, both gaseous and particulate PAHs in winter could be affected by emission sources in northeastern China.

In spring, CWT highlighted that the particulate Σ_{21} PAHs including BaP in Ulsan could be contributed by those originating from eastern China (i.e., Hebei and Shandong), North Korea, and South Korea (Figure 15). On the other hand, the gaseous Σ_{21} PAHs in Ulsan might be affected by different region, suggesting the gaseous Σ_{21} PAHs could be originated from northeastern and eastern China (i.e., Jilin, Inner Mongolia, Liaoning, and Jiangsu) and southern South Korea. However, surface winds showed that prevailing winds in spring passed over industrial areas before arriving sampling site (Figure 3b). Therefore, gaseous and particulate PAHs in spring could be contributed by those emitted from local and regional sources.

In summer, CWT revealed that Σ_{21} PAHs in both gaseous and particulate phases were driven from eastern China (i.e., Shandong), South Korea, and Japan (Figure 16). Specially, South Korea and Japan might contribute to the particulate BaP in Ulsan. However, prevailing seasonal wind (i.e., southeasterly wind) could transport PAHs emitted from industrial area to the sample site (Figure 3c). Moreover, relatively low wind speed in summer could cause the low air dispersion, resulting in greater contributions from local sources. This is consistent with results from previous studies (Nguyen, 2020).

Previous studies reported that particulate PAHs emitted from northern (i.e., Liaoning), northeastern (i.e., Hebei and Beijing), and eastern China (i.e., Shandong) and North Korea could contribute to those in Seoul (Kim et al., 2016b; Kim et al., 2016c). In winter, CWT result in Ulsan is in line with results from previous studies investigated in Seoul. In spring, on the contrary, eastern China (i.e., Hebei and

Shandong) and southeastern North Korea could more contribute to the particulate Σ_{21} PAHs in Ulsan and were more highlighted in CWT. Moreover, CWT in summer highlighted that emission sources from South Korea and Japan could affect to the particulate PAHs in Ulsan. Consequently, levels of PAHs including BaP in winter and spring could be attributable both regional sources (i.e., northern and northeastern China, North Korea in winter and northeastern and eastern China and North Korea in spring) as well as local emission sources, whereas those in summer could be primarily derived from local emission sources.
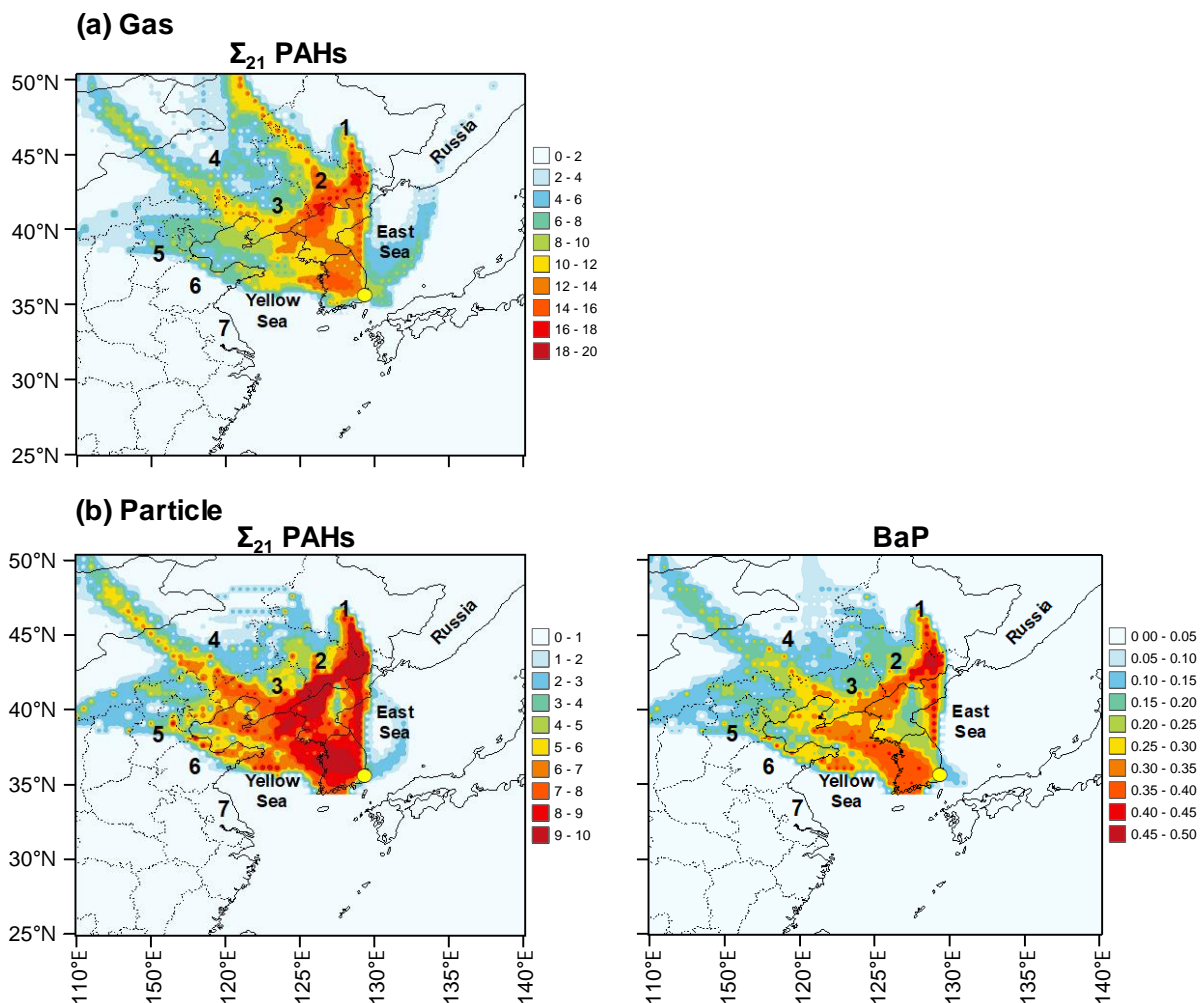
Figure 14. CWT of Σ_{21} PAHs and BaP in (a) the gaseous and (b) particulate phases in winter. The numbers indicate several areas in China; Heilongjiang (1), Jilin (2), Liaoning (3), Inner Mongolia (4), Hebei (5), Shandong (6), Jiangsu (7).
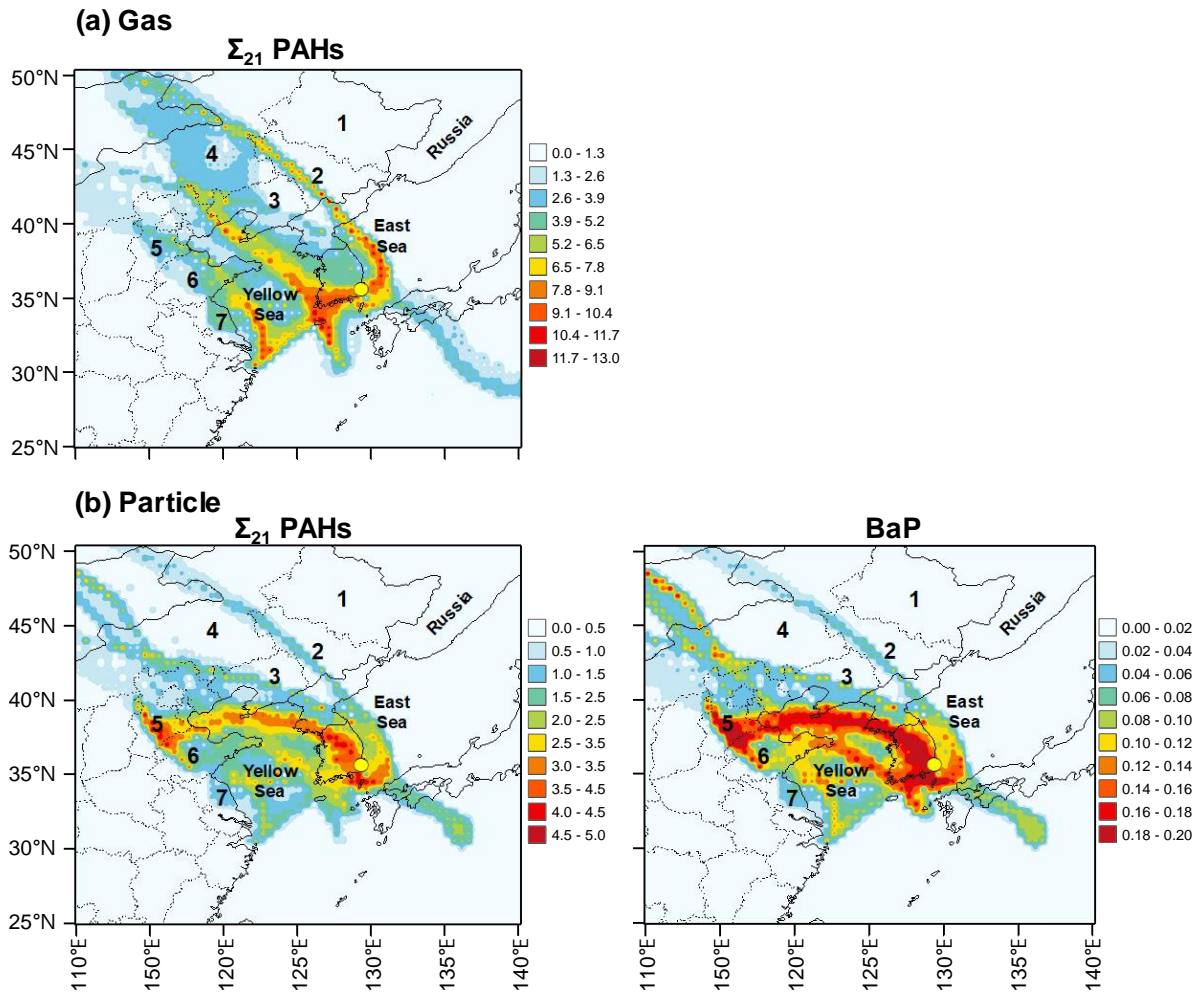
Figure 15. CWT of Σ_{21} PAHs and BaP in (a) the gaseous and (b) particulate phases in spring. The numbers indicate several areas in China; Heilongjiang (1), Jilin (2), Liaoning (3), Inner Mongolia (4), Hebei (5), Shandong (6), Jiangsu (7).
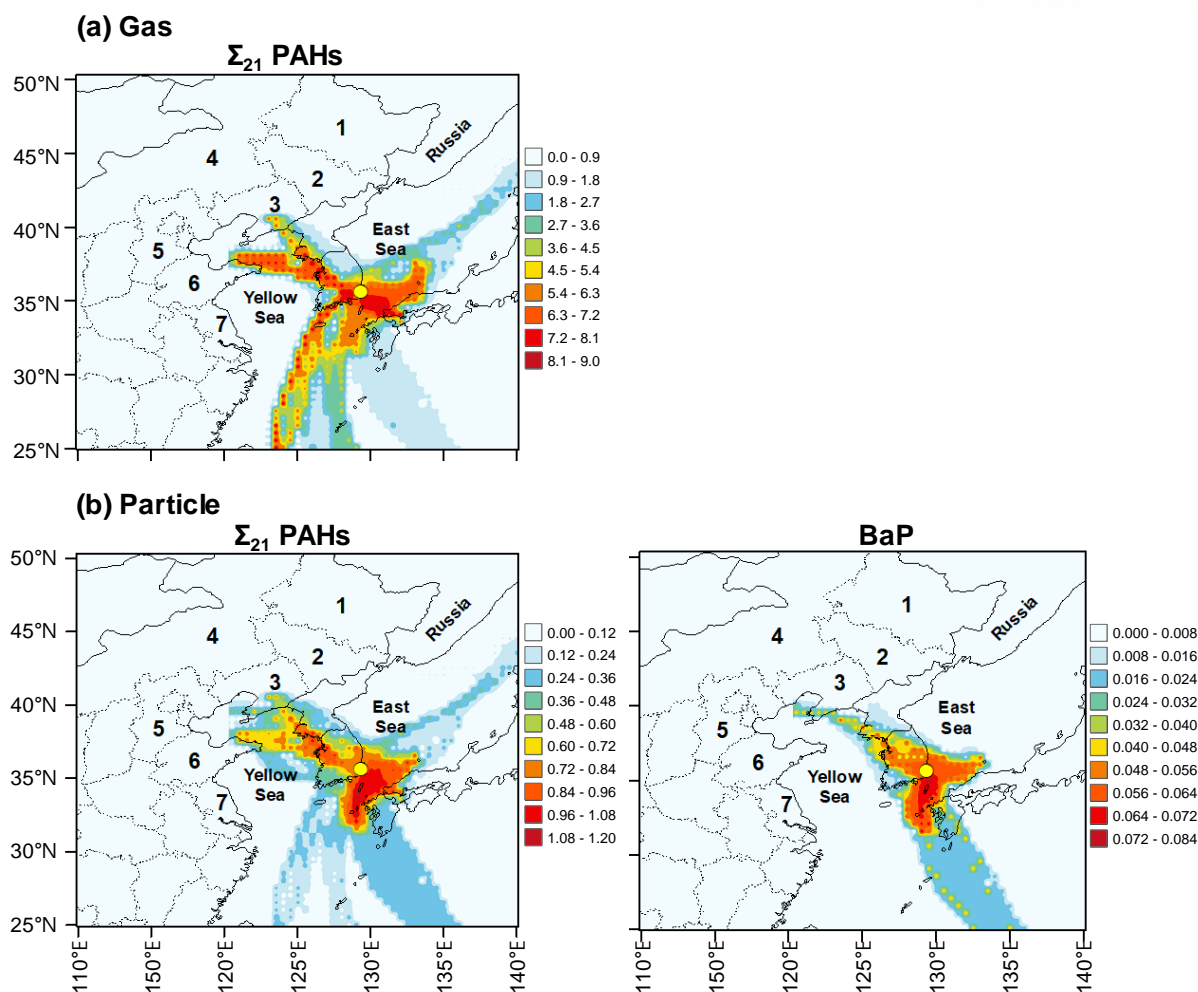
Figure 16. CWT of Σ_{21} PAHs and BaP in (a) the gaseous and (b) particulate phases in summer. The numbers indicate several areas in China; Heilongjiang (1), Jilin (2), Liaoning (3), Inner Mongolia (4), Hebei (5), Shandong (6), Jiangsu (7).

In summary, in winter, the both gaseous and particulate PAHs in Ulsan could be affected by pyrogenic sources (i.e., coal and biomass burning) and natural gas burning sources in local and reginal areas (i.e., northern and northeastern China (i.e., Heilongjiang, Jilin, Liaoning, Inner Mongolia, Hebei, and Shandong) and North Korea). In spring, the gaseous PAHs originated from incineration source and lubricating oil combustion at eastern and northeastern China as well as local emission sources could contribute to those at Ulsan. On the contrary, the particulate PAHs in spring could be affected by natural gas combustion and coal combustion sources from eastern China (i.e., Hebei and Shandong) and North Korea. In summer, both gaseous and particulate PAHs could be strongly affected by local emission sources, especially, industrial areas in Ulsan.

3.3 Health risk assessment

The total Σ_{21} BaP$_{eq}$ concentrations and their phase distributions are presented in Figure 17a. The Σ_{21} BaP$_{eq}$ showed the highest concentration in winter (mean: 0.60 ng/m^3), followed by spring (mean: 0.27 ng/m^3) and summer (mean: 0.17 ng/m^3) since PAH concentrations and fraction of 5- and 6-ring were highest in winter and lowest in summer (as described in Section 3.1). In addition, the particulate concentrations of Σ_{21} BaP$_{eq}$ were higher than the Σ_{21} BaP$_{eq}$ concentrations of gaseous PAHs (winter: 17 times, spring: 6.7 times, and summer: 3.5 times). The mean Σ_{13} BaP$_{eq}$ concentrations in total (gaseous + particulate) phase were 0.48, 0.22, and 0.11 ng/m^3 in winter, spring, and summer, respectively. These BaP$_{eq}$ concentrations of Σ_{13} PAHs showed similar with those in urban areas and lower than those in semi-rural and industrial areas in Ulsan (Nguyen et al., 2020). In addition, the average Σ_{13} BaP$_{eq}$ concentrations in Ulsan is generally lower than those in industrial area in Taiwan (Liu et al., 2010), urban areas in Beijing and Tenjin, China (Chao et al., 2019; Han et al., 2016).

Among the Σ_{21} BaP$_{eq}$, the Σ_8 BaP$_{eq}$ which consist BjF, DMBA, 3MCA, DbaiP, DbahP, and DbalP contributed 21%, 19%, and 36% in winter, spring, and summer, respectively (Figure 17b). Figure 18 illustrates concentrations and profiles of Σ_{21} BaP$_{eq}$ in the gaseous, particulate, and total (gaseous + particulate) phases. In winter, the major contributions to total gaseous Σ_{21} BaP$_{eq}$ came from DbahP (24%), BaP (23%), and Phe (14%), and those to total particulate Σ_{21} BaP$_{eq}$ came from BaP (43%), DbahP (16%), and Ind (9%). In spring, BaP (gas: 49% and particle: 44%), DahA (gas: 11% and particle: 10%), and Ind (gas: 10% and particle: 9%) were the most abundant compounds in the both gaseous and particulate phases. In summer, Σ_{21} BaP$_{eq}$ in the gaseous phase was mainly contributed by BaP (51%), DbaiP (17%), and Phe (10%), and Σ_{21} BaP$_{eq}$ in the particulate phase was mainly contributed by BaP (30%), DbaiP (27%), and DahA (19%). Especially, DbaiP and DbahP accounted for 31% of the gaseous Σ_{21} BaP$_{eq}$ and 16% of the particulate Σ_{21} BaP$_{eq}$. Although DbaiP and DbahP showed low contributions in the total Σ_{21} PAHs in the atmosphere (0.02% and 0.04%, respectively), they showed the high contributions in BaP$_{eq}$ (6% and 12%, respectively) due to their high TEF values (Table 1). Hong et al. (2020) suggested that the contribution of dibenzopyrenes (i.e., DbaiP, DbahP, DbalP, and dibenzo[a,e]pyrene (DbaeP)) accounted for 28% of the total Σ_{53} BaP$_{eq}$ concentration although they comprised 0.8% of the 53 PAHs. Additionally, DbaiP, DbahP, and DbalP in particulate matter (PM) resulted in the increase of total BaP$_{eq}$ concentration (Layshock et al., 2010; Wang et al., 2016). Therefore, this finding could suggest that PAHs having high TEF values (i.e., DbaiP, DbahP, and DbalP) could play important roles in levels of BaP$_{eq}$ and risk.
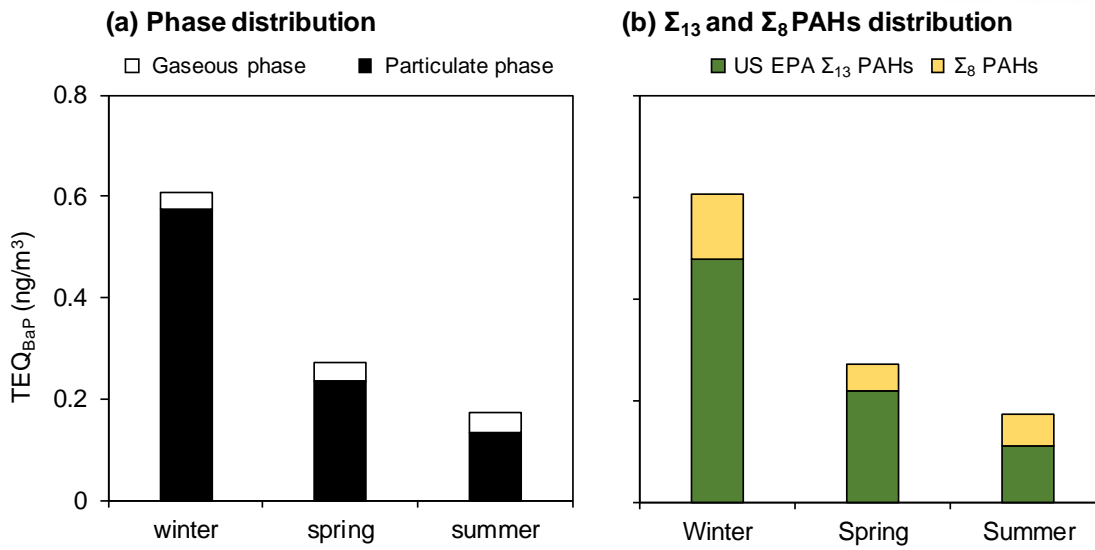
Figure 17. Mean concentrations of BaP_{eq} in three seasons: (a) phase distribution of Σ_{21} BaP_{eq} and (b) distribution of Σ_8 BaP_{eq} and Σ_{13} BaP_{eq} in total (gaseous + particulate) phase.
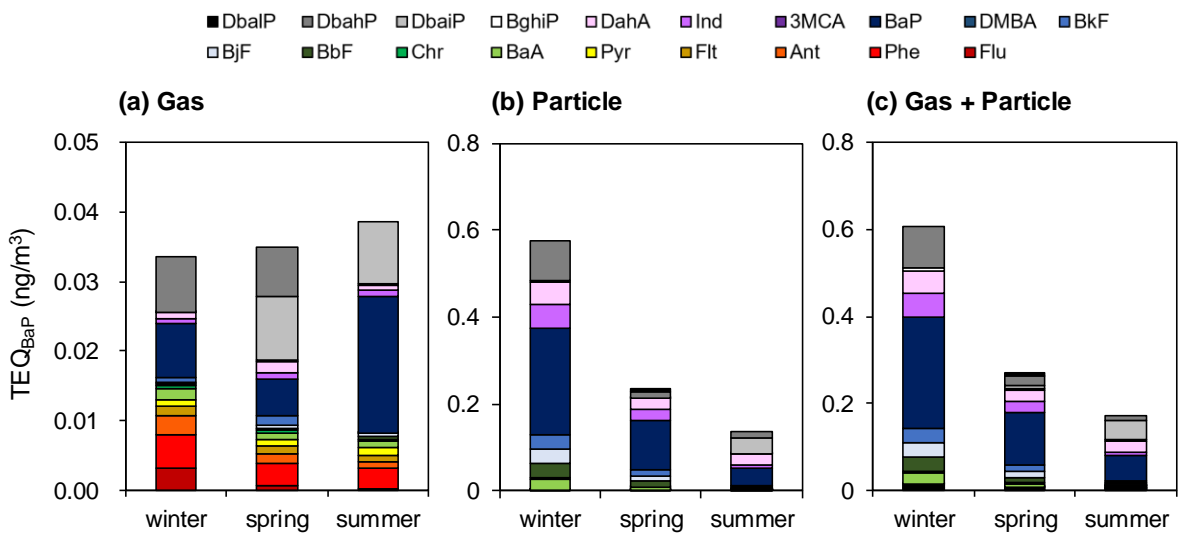
Figure 18. Concentration and profiles of Σ_{21} BaP_{eq} over three seasons in (a) the gaseous, (b) particulate, and (c) total (gaseous + particulate) phases.

Figure 19 shows the annual cancer risk for the Σ_{13} and the total Σ_{21} PAHs. As shown in Figure 20, the range of the total (gas + particle) cancer risk for the Σ_{13} PAHs were 2.45×10^{-8}–4.85×10^{-7} in winter, 2.45×10^{-8}–4.85×10^{-7} in spring, and 2.45×10^{-9}–4.85×10^{-8} in summer, respectively. This result was similar with the previous study in Ulsan (Nguyen et al., 2020). The range of the total (gas + particle) cancer risk for the Σ_{21} PAHs were 3.28×10^{-8}–6.33×10^{-7} in winter, 1.36×10^{-8}–2.41×10^{-7} in spring, and 8.80×10^{-9}–1.72×10^{-7} in summer. Both cancer risk of Σ_{13} and Σ_{21} PAHs were lower than the acceptable risk level (10^{-6}) suggested by US EPA. However, ILCRs of the total Σ_{21} PAHs were 1.2 to 1.6 times higher than those of Σ_{13} PAHs, because the BaP_{eq} concentrations between the Σ_{13} and the total Σ_{21} PAHs are different. In other words, the high TEF values of PAHs, that are not listed by US EPA (i.e., DbaiP, DbahP, and DbalP), increased BaP_{eq} and cancer risk. Previous studies also highlighted the risk of dibenzopyrenes in the atmosphere due to their high toxicities (Hong et al., 2020; Layshock et al., 2010). Therefore, it is important to investigate the toxicity of other PAHs over the US EPA priority PAHs and their health risk evaluation in further studies.

(a) Σ_{13} PAHs
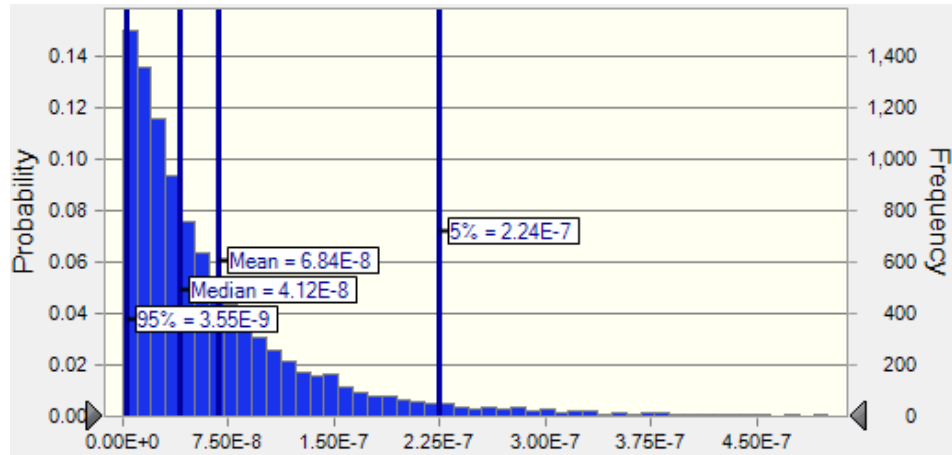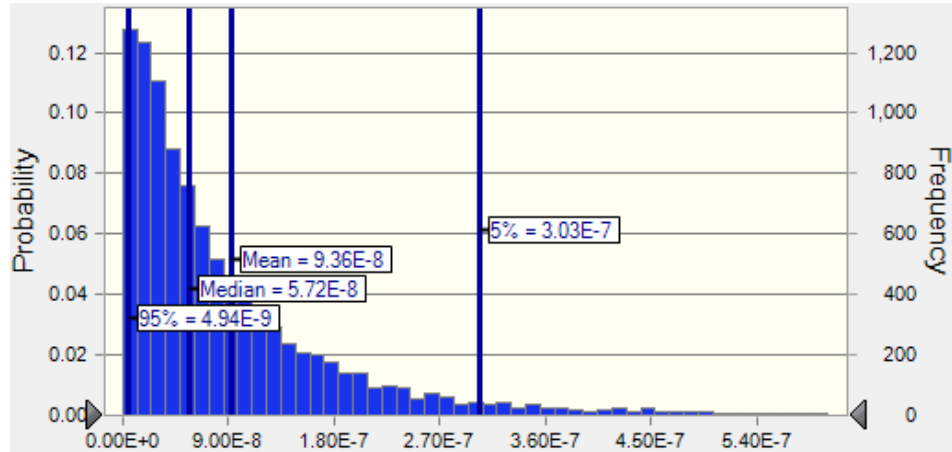
(b) Σ_{21} PAHs

Figure 19. Probability density functions of the annual cancer risk for (a) the Σ_{13} PAHs and (b) Σ_{21} PAHs during sampling seasons.
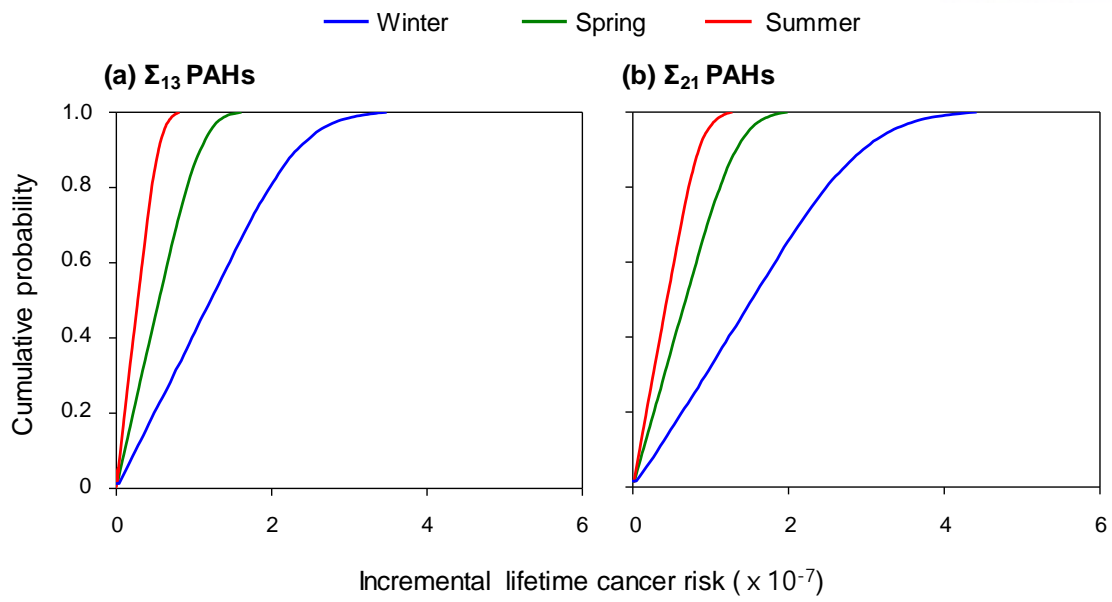
Figure 20. Cumulative probability ILCR of (a) Σ_{13} PAHs and (b) Σ_{21} PAHs through inhalation for three seasons.

IV. CONCLUSION

This study identified seasonal variation of 21 PAHs in ambient air in Ulsan, South Korea. The PAH concentrations were mainly highest in winter and lowest in summer. The 3- and 4-ring species were dominant in the gaseous phase and 4-, 5-, and 6- ring PAHs were dominant in particulate phase. Also, high concentration of PAHs in winter indicates the increased PAH emission and low dispersion due to low mixing layer. Moreover, the contribution of the Σ_8 PAHs which are not listed at the priority PAHs to the Σ_{21} PAH were 5.2% and they were mostly partitioned in the particulate phase.

The emission sources of PAHs were various in three seasons. PAHs in winter were mainly influenced by pyrogenic sources including coal/biomass and natural gas burning, reflecting combustion for residential heating. On the other hand, PAHs in summer were affected by petrogenic and petroleum combustion sources emitted from industrial areas in Ulsan by seasonal winds (i.e., southeasterly wind). PAHs in spring were affected by both petrogenic and pyrogenic sources. Moreover, The BeP/BaP ratio suggested that PAHs in Ulsan could be affected by long-range transport in winter and spring. According to the hybrid receptor model (i.e., CWT), PAHs in winter and spring could be more contributed by those originated from regional emission sources as well as local sources, whereas PAHs in summer mostly affected by the local sources. Therefore, PAHs in winter and spring might be affected by pyrogenic sources (i.e., coal/biomass and natural gas burning) from the both regional and local areas. The PAHs in summer might be affected by both petrogenic and pyrogenic sources in local areas, especially industrial areas in Ulsan.

This study firstly conducted the risk assessment of PAHs considering the more toxic species than BaP in South Korea. The estimated cancer risk Σ_{21} PAHs were higher than those of US EPA priority Σ_{13} PAHs. The high TEF values of DbaiP and DbahP affected the increase of cancer risk in spite of low concentrations in the atmosphere.

This is preliminary study to understand the pollution characteristics and cancer risk of atmospheric PAHs, which have high toxicity, in South Korea. PAHs in Ulsan could be contributed by both local emission and long-range transport. Indeed, toxic PAH species played important roles to human health due to their high potential carcinogenicities. Based on this study, further studies should more focus on the toxic PAHs in multimedia environment (e.g., atmosphere, soil, and water etc.) to understand the transport behavior and fate of the PAHs.

Akyuz, M., and Cabuk, H. (2010). Gas-particle partitioning and seasonal variation of polycyclic aromatic hydrocarbons in the atmosphere of Zonguldak, Turkey. *Science of the Total Environment, 408*(22), 5550-5558.

Andersson, J. T., and Achten, C. (2015). Time to say goodbye to the 16 EPA PAHs? Toward an up-to-date use of PACs for environmental purposes. *Polycyclic Aromatic Compounds, 35*(2-4), 330-354.

Arinaitwe, K., Kiremire, B. T., Muir, D. C., Fellin, P., Li, H., Teixeira, C., and Mubiru, D. N. (2012). Atmospheric concentrations of polycyclic aromatic hydrocarbons in the watershed of Lake Victoria, East Africa. *Environmental Science & Technology, 46*(21), 11524-11531.

Baek, S. O., Field, R. A., Goldstone, M. E., Kirk, P. W., Lester, J. N., and Perry, R. (1991). A review of atmospheric polycyclic aromatic hydrocarbons: sources, fate and behavior. *Water, Air, & Soil Pollution, 60*(3-4), 279-300.

CalEPA. (2009). Technical support document for cancer potency factors: Methodologies for derivation, listing of available values and adjustments to allow for early life stage exposures.

Chao, S., Liu, J., Chen, Y., Cao, H., and Zhang, A. (2019). Implications of seasonal control of PM2.5-bound PAHs: An integrated approach for source apportionment, source region identification and health risk assessment. *Environmental Pollution, 247*, 685-695.

Chen, S. C., and Liao, C. M. (2006). Health risk assessment on human exposed to environmental polycyclic aromatic hydrocarbons pollution sources. *Science of the Total Environment, 366*(1), 112-123.

Choi, S.-D., Ghim, Y. S., Lee, J. Y., Kim, J. Y., and Kim, Y. P. (2012a). Factors affecting the level and pattern of polycyclic aromatic hydrocarbons (PAHs) at Gosan, Korea during a dust period. *Journal of hazardous materials, 227-228*, 79-87.

Choi, S.-D., Kwon, H.-O., Lee, Y.-S., Park, E.-J., and Oh, J.-Y. (2012b). Improving the spatial resolution of atmospheric polycyclic aromatic hydrocarbons using passive air samplers in a multi-industrial city. *Journal of hazardous materials, 241*, 252-258.

Clarke, K., Kwon, H.-O., and Choi, S.-D. (2014). Fast and reliable source identification of criteria air pollutants in an industrial city. *Atmospheric environment, 95*, 239-248.

Cohen, Y., and Clay, R. E. (1994). Multimedia partitioning of particle-bound organics. *Journal of hazardous materials, 37*, 507-526.

Collins, J. F., Brown, J. P., Alexeeff, G. V., and Salmon, A. G. (1998). Potency Equivalency Factors for Some Polycyclic Aromatic Hydrocarbons and Polycyclic Aromatic Hydrocarbon Derivatives. *Regulatory Toxicology and Pharmacology, 28*, 45-54.

da Silva, D. A., and Bícego, M. C. (2010). Polycyclic aromatic hydrocarbons and petroleum biomarkers in São Sebastião Channel, Brazil: assessment of petroleum contamination. *Marine environmental research, 69*(5), 277-286.

Daisey, J. M., Cheney, J. L., and Lioy, P. J. (1986). Profiles of organic particulate emissions from air pollution sources: status and needs for receptor source apportionment modeling. *Journal of the Air Pollution Control Association, 36*(1), 17-33.

de Andrade, S. J., Cristale, J., Silva, F. S., Julião Zocolo, G., and Marchi, M. R. R. (2010). Contribution of sugar-cane harvesting season to atmospheric contamination by polycyclic aromatic

hydrocarbons (PAHs) in Araraquara city, Southeast Brazil. *Atmospheric environment, 44*(24), 2913-2919.

Esen, F., Tasdemir, Y., and Vardar, N. (2008). Atmospheric concentrations of PAHs, their possible sources and gas-to-particle partitioning at a residential site of Bursa, Turkey. *Atmospheric Research, 88*(3-4), 243-255.

Fakhri, Y., Mousavi Khaneghah, A., Conti, G. O., Ferrante, M., Khezri, A., Darvishi, A., Ahmadi, M., Hasanzadeh, V., Rahimizadeh, A., Keramati, H., Moradi, B., and Amanidaz, N. (2018). Probabilistic risk assessment (Monte Carlo simulation method) of Pb and Cd in the onion bulb (Allium cepa) and soil of Iran. *Environmental Science and Pollution Research, 25*(31), 30894-30906.

Fang, G.-C., Wu, Y.-S., Chen, M.-H., Ho, T.-T., Huang, S.-H., and Rau, J.-Y. (2004). Polycyclic aromatic hydrocarbons study in Taichung, Taiwan, during 2002-2003. *Atmospheric environment, 38*(21), 3385-3391.

Han, B., Liu, Y., You, Y., Xu, J., Zhou, J., Zhang, J., Niu, C., Zhang, N., He, F., Ding, X., and Bai, Z. (2016). Assessing the inhalation cancer risk of particulate matter bound polycyclic aromatic hydrocarbons (PAHs) for the elderly in a retirement community of a mega city in North China. *Environmental Science and Pollution Research, 23*(20), 20194-20204.

Harkov, R., and Greenberg, A. (1985). Benzo(a)pyrene in New Jersey--results from a twenty-seven-site study. *Journal of the Air Pollution Control Association, 35*(3), 238-243.

Hong, W. J., Jia, H., Yang, M., and Li, Y. F. (2020). Distribution, seasonal trends, and lung cancer risk of atmospheric polycyclic aromatic hydrocarbons in North China: A three-year case study in Dalian city. *Ecotoxicological Environmental Safety, 196*, 110526.

Hsu, Y.-K., Holsen, T. M., and Hopke, P. K. (2003). Comparison of hybrid receptor models to locatePCB sources in Chicago. *Atmospheric environment, 37*, 545-562.

Hsu, Y.-M., Harner, T., Li, H., and Fellin, P. (2015). PAH Measurements in Air in the Athabasca Oil Sands Region. *Environmental Science & Technology, 49*(9), 5584-5592.

Huang, X.-F., He, L.-Y., Hu, M., and Zhang, Y.-H. (2006). Annual variation of particulate organic compounds in PM2.5 in the urban atmosphere of Beijing. *Atmospheric environment, 40*(14), 2449-2458.

IARC. (2004). IARC monographs on the evaluation of carcinogenic risks to humans. *Lyon, France*, 1-1452.

IARC. (2010). IARC Monographs on the Evaluation of Carcinogenic Risks to humans. *Some Non-heterocyclic PolycyclicAromatic Hydrocarbons and Some Related Exposures, 92*, 1-868.

IARC. (2012). Chemical agents and related occupations. *Lyon, France., 100*(PT F), 9.

Ichikawa, Y., Watanabe, T., Horimoto, Y., Ishii, K., and Naito, S. (2018). Measurements of 50 Non-polar Organic Compounds Including Polycyclic Aromatic Hydrocarbons, n-Alkanes and Phthalate Esters in Fine Particulate Matter (PM2.5) in an Industrial Area of Chiba Prefecture, Japan. *Asian Journal of Atmospheric Environment, 12*(3), 274-288.

Kim, B. M., Lee, S. B., Kim, J. Y., Kim, S., Seo, J., Bae, G. N., and Lee, J. Y. (2016a). A multivariate receptor modeling study of air-borne particulate PAHs: Regional contributions in a roadside environment. *Chemosphere, 144*, 1270-1279.

Kim, B. M., Seo, J., Kim, J. Y., Lee, J. Y., and Kim, Y. (2016b). Transported vs. local contributions from secondary and biomass burning sources to PM2.5. *Atmospheric environment, 144*, 24-36.

Kim, I. S., Wee, D., Kim, Y. P., and Lee, J. Y. (2016c). Development and application of three-dimensional potential source contribution function (3D-PSCF). *Environmental Science and Pollution Research, 23*(17), 16946-16954.

Kiss, G., Varga-Puchony, Z., Rohrbacher, G., and Hlavay, J. (1998). Distribution of polycyclic aromatic hydrocarbons on atmospheric aerosol particles of different sizes. *Atmospheric Research, 46*(3-4), 153-261.

Kulkarni, P., and Venkataraman, C. (2000). Atmospheric polycyclic aromatic hydrocarbons in Mumbai, India. *Atmospheric environment, 34*(17), 2785-2790.

Kume, K., Ohura, T., Noda, T., Amagai, T., and Fusaya, M. (2007). Seasonal and spatial trends of suspended-particle associated polycyclic aromatic hydrocarbons in urban Shizuoka, Japan. *Journal of hazardous materials, 144*(1-2), 513-521.

Layshock, J., Simonich, S. M., and Anderson, K. A. (2010). Effect of dibenzopyrene measurement on assessing air quality in Beijing air and possible implications for human health. *Journal of Environmental Monitoring, 12*(12), 2290-2298.

Lee, J. Y., Kim, Y. P., and Kang, C.-H. (2011). Characteristics of the ambient particulate PAHs at Seoul, a mega city of Northeast Asia in comparison with the characteristics of a background site. *Atmospheric Research, 99*(1), 50-56.

Lee, J. Y., Kim, Y. P., Kang, C.-H., Ghim, Y. S., and Kaneyasu, N. (2006). Temporal trend and long-range transport of particulate polycyclic aromatic hydrocarbons at Gosan in northeast Asia between 2001 and 2004. *Journal of Geophysical Research, 111*(D11).

Lee, J. Y., Shin, H. J., Bae, S. Y., Kim, Y. P., and Kang, C.-H. (2008). Seasonal variation of particle size distributions of PAHs at Seoul, Korea. *Air Quality, Atmosphere & Health, 1*(1), 57-68.

Liu, H. H., Yang, H. H., Chou, C. D., Lin, M. H., and Chen, H. L. (2010). Risk assessment of gaseous/particulate phase PAH exposure in foundry industry. *Journal of hazardous materials, 181*(1-3), 105-111.

Mackay, D., Shiu, W.-Y., Ma, K.-C., and Lee, S. C. (2006a). *Handbook of physical-chemical properties and environmental fate for organic chemicals*: CRC press.

Mackay, D., Shiu, W.-Y., Ma, K.-C., and Lee, S. C. (2006b). *Handbook of physical-chemical properties and environmental fate for organic chemicals Volume I: Introduction and hydrocarbons*: CRC press.

Masala, S., Lim, H., Bergvall, C., Johansson, C., and Westerholm, R. (2016). Determination of semi-volatile and particle-associated polycyclic aromatic hydrocarbons in Stockholm air with emphasis on the highly carcinogenic dibenzopyrene isomers. *Atmospheric environment, 140*, 370-380.

Masih, J., Dyavarchetty, S., Nair, A., Taneja, A., and Singhvi, R. (2019). Concentration and sources of fine particulate associated polycyclic aromatic hydrocarbons at two locations in the western coast of India. *Environmental Technology & Innovation, 13*, 179-188.

MOE. (2007). Korean eposure factors handbook.

Mostert, M. M. R., Ayoko, G. A., and Kokot, S. (2010). Application of chemometrics to analysis of soil pollutants. *TrAC Trends in Analytical Chemistry, 29*(5), 430-445.

Nguyen, T. N. T. (2020). *MULTIMEDIA MONITORING OF POLYCYCLIC AROMATIC HYDRCARBONS (PAHs) IN A LARGE INDUSTRIAL CITY: PHASE DISTRIBUTION AND EMISSION SOURCE IDENTIFICATION.* (degree of Doctor of Philosophy Doctoral Dissertation). Ulsan National Institute of Science and Technology, Graduate School of UNIST. (1-144)

Nguyen, T. N. T., Jung, K.-S., Son, J. M., Kwon, H.-O., and Choi, S.-D. (2018). Seasonal variation, phase distribution, and source identification of atmospheric polycyclic aromatic hydrocarbons at a semi-rural site in Ulsan, South Korea. *Environmental Pollution, 236*, 529-539.

Nguyen, T. N. T., Kwon, H. O., Lammel, G., Jung, K. S., Lee, S. J., and Choi, S. D. (2020). Spatially high-resolved monitoring and risk assessment of polycyclic aromatic hydrocarbons in an industrial city. *Journal of hazardous materials, 393*, 122409.

NIER. (2016a). Korean exposure factors handbook for children.

NIER. (2016b). Monitoring of Hazardous Air Pollutants in the Industrial Ambient Atmosphere(II).

NIER. (2018). Monitoring of Hazardous Air Pollutants in the Urban Ambient Atmosphere(IV).

NIER. (2019). Monitoring of Hazardous Air Pollutants in the Urban Ambient Atmosphere(V).

Nisbet, I. C. T., and Lagoy, P. K. (1992). Toxic equivalency factors (TEFs) for polycyclic aromatic hydrocarbons (PAHs). *Regulatory Toxicology and Pharmacology, 16*(3), 290-300.

OEHHA. (1994). BENZO[a]PYRENE AS A TOXIC AIR CONTAMINANT.

Ren, Y., Zhou, B., Tao, J., Cao, J., Zhang, Z., Wu, C., Wang, J., Li, J., Zhang, L., Han, Y., Liu, L., Cao, C., and Wang, G. (2017). Composition and size distribution of airborne particulate PAHs and oxygenated PAHs in two Chinese megacities. *Atmospheric Research, 183*, 322-330.

Rogge, W. F., Hildemann, L. M., Mazurek, M. A., Cass, G. R., and Simoneit, B. R. T. (1993). Sources of fine organic aerosol. 2. Noncatalyst and catalyst-equipped automobiles and heavy-duty diesel trucks. *Environmental Science & Technology, 27*(4), 636-651.

Simcik, M. F., Eisenreich, S. J., and Lioy, P. J. (1999). Source apportionment and source/sink relationships of PAHs in the coastal atmosphere of Chicago and Lake Michigan. *Atmospheric environment, 33*(30), 5071-5079.

Simoneit, B. R. T. (2002). Biomass burning — a review of organic tracers for smoke from incomplete combustion. *Applied Geochemistry, 17*(3), 129-162.

Sofuoglu, S. C., Sofuoglu, A., Holsen, T. M., Alexander, C. M., and Pagano, J. J. (2013). Atmospheric concentrations and potential sources of PCBs, PBDEs, and pesticides to Acadia National Park. *Environmental Pollution, 177*, 116-124.

Tang, L., Haeger-Eugensson, M., Sjöberg, K., Wichmann, J., Molnár, P., and Sallsten, G. (2014). Estimation of the long-range transport contribution from secondary inorganic components to urban background PM10 concentrations in south-western Sweden during 1986–2010. *Atmospheric environment, 89*, 93-101.

Thang, P. Q., Kim, S.-J., Lee, S.-J., Ye, J., Seo, Y.-K., Baek, S.-O., and Choi, S.-D. (2019). Seasonal characteristics of particulate polycyclic aromatic hydrocarbons (PAHs) in a petrochemical and oil refinery industrial area on the west coast of South Korea. *Atmospheric environment, 198*, 398-406.

US-EPA. (1993). Provisional guidance for quantitative risk assessment of polycyclic aromatic hydrocarbons. 1-28.

Wang, Q., Kobayashi, K., Lu, S., Nakajima, D., Wang, W., Zhang, W., Sekiguchi, K., and Terasaki, M. (2016). Studies on size distribution and health risk of 37 species of polycyclic aromatic hydrocarbons associated with fine particulate matter collected in the atmosphere of a suburban area of Shanghai city, China. *Environmental Pollution, 214*, 149-160.

Wang, Y. Q., Zhang, X. Y., and Draxler, R. R. (2009). TrajStat: GIS-based software that uses various trajectory statistical analysis methods to identify potential sources from long-term air pollution measurement data. *Environmental Modelling & Software, 24*(8), 938-939.

Yunker, M. B., Macdonald, R. W., Vingarzan, R., Mitchell, R. H., Goyette, D., and Sylvestrec, S. (2002). PAHs in the Fraser River basin: a critical appraisal of PAH ratios as indicators of PAH source and composition. *Organic Geochemistry, 33*(4), 489-515.

Zhang, Y., Chen, J., Yang, H., Li, R., and Yu, Q. (2017). Seasonal variation and potential source regions of PM2.5-bound PAHs in the megacity Beijing, China: Impact of regional transport. *Environmental Pollution, 231*(Pt 1), 329-338.
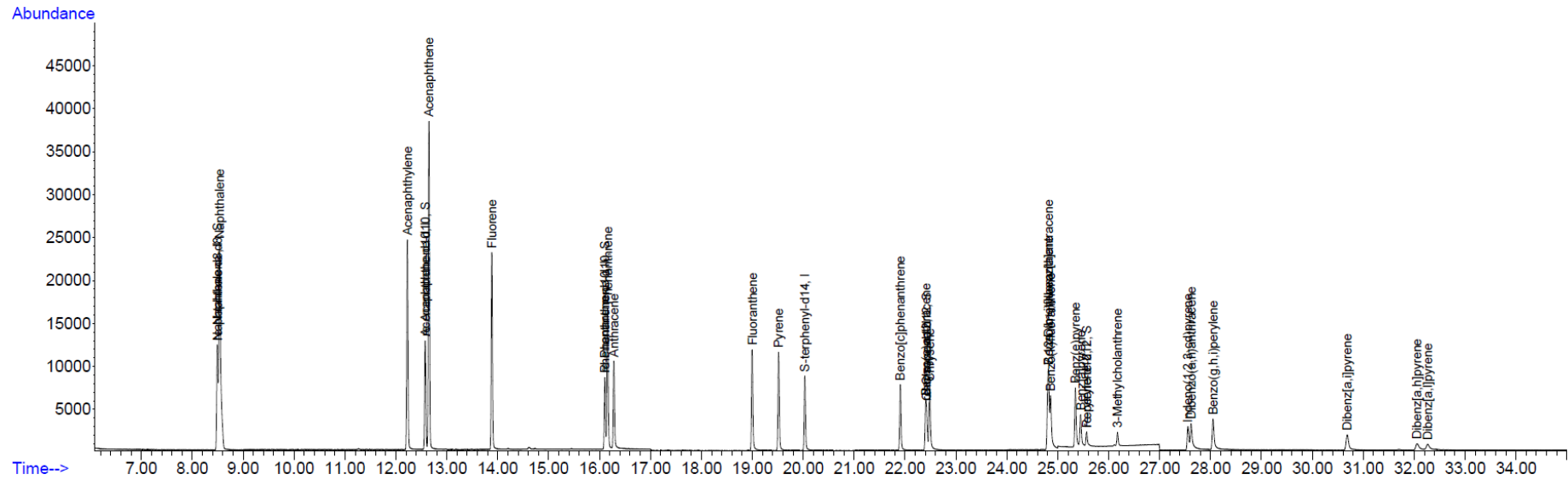
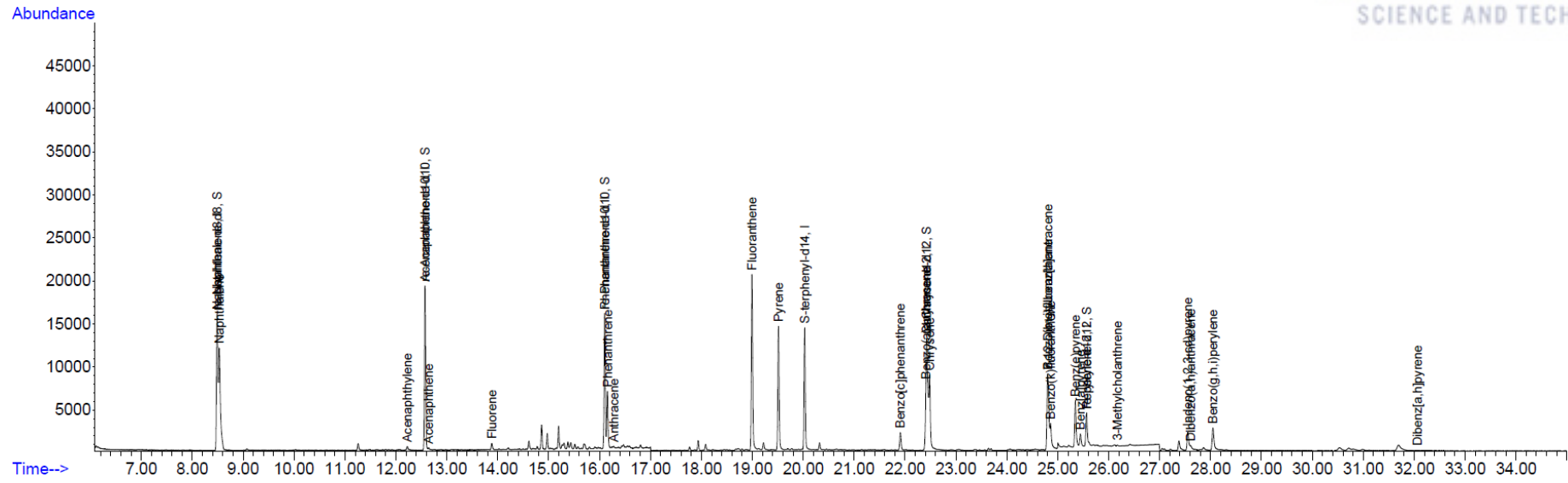**Figure 20.** Chromatogram of the standard solution of 24 PAHs standard.

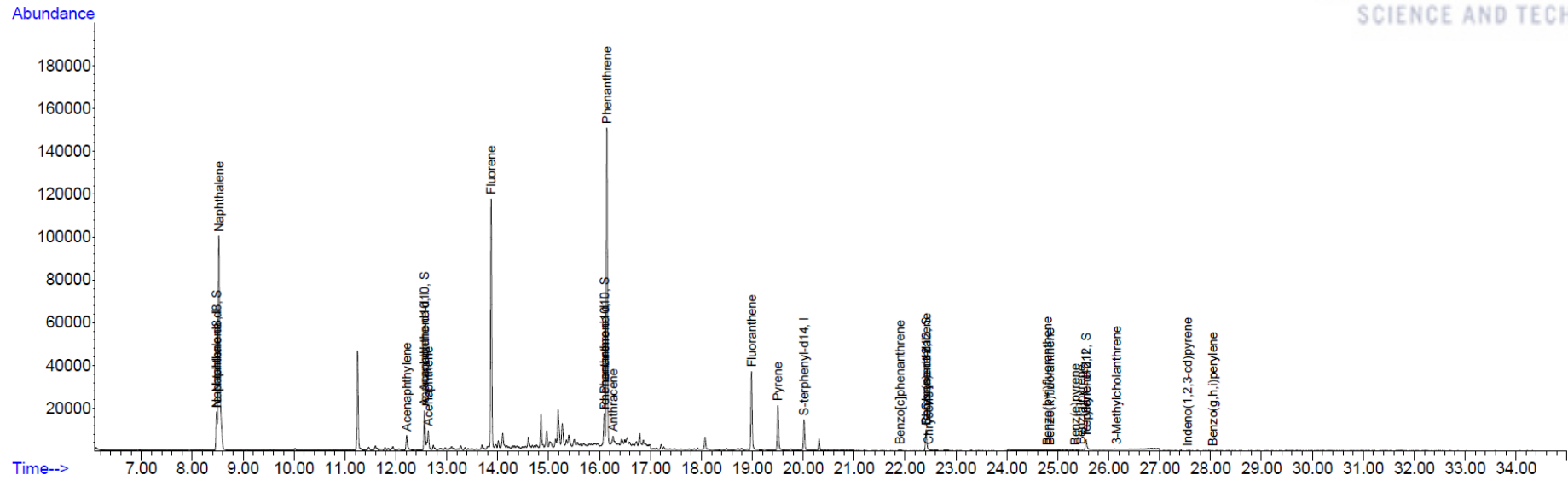**Figure 21.** Chromatogram of the 24 PAHs in GFF sample.

Figure 22. Chromatogram of the 24 PAHs in PUF sample.

Table 11. Concentrations (ng/m^3) of the particulate 21 PAHs during sampling period.

	WT1	WT2	WT3	WT4	WT5	WT6	WT7	WT8	WT9	WT10	SP1	SP2	SP3	SP4	SP5	SP6	SP7	SP8	SP9	SP10	SP11	SU1	SU2	SU3	SU4	SU5	SU6	SU7	SU8	SU9	SU10	SU11
Flu	N.D.	N.D.	<MDL	N.D.	N.D.	N.D.	<MDL	<MDL	N.D.	<MDL	N.D.	<MDL	<MDL	N.D.	N.D.	<MDL	N.D.	N.D.	N.D.	N.D.	N.D.	N.D.	N.D.	N.D.	N.D.	N.D.	N.D.	N.D.	<MDL	<MDL	<MDL	0.04
Phe	<MDL	N.D.	0.79	0.39	0.10	<MDL	0.41	0.08	N.D.	0.15	0.08	0.15	<MDL	0.06	0.21	0.07	<MDL	<MDL	0.12	0.07	<MDL	N.D.	N.D.	<MDL	<MDL	0.09	N.D.	<MDL	<MDL	0.07	0.05	0.17
Ant	<MDL	<MDL	<MDL	<MDL	N.D.	N.D.	<MDL	<MDL	N.D.	<MDL	N.D.	<MDL	<MDL	N.D.	N.D.	<MDL	N.D.	N.D.	<MDL	N.D.	N.D.	<MDL	N.D.	<MDL	<MDL	<MDL	N.D.	<MDL	<MDL	<MDL	<MDL	<MDL
Flt	0.09	<MDL	2.28	1.41	1.12	1.32	2.12	0.23	0.35	0.23	0.64	<MDL	<MDL	0.17	0.74	0.17	<MDL	0.15	0.39	0.20	0.28	<MDL	<MDL	<MDL	0.09	0.22	<MDL	0.09	<MDL	0.12	<MDL	<MDL
Pyr	0.10	<MDL	1.77	1.06	0.96	1.04	1.51	0.19	0.28	0.17	0.54	0.08	<MDL	0.19	0.62	0.13	<MDL	0.12	0.31	0.15	0.23	<MDL	<MDL	<MDL	0.09	0.18	<MDL	0.08	<MDL	0.10	<MDL	<MDL
BcPhe	<MDL	<MDL	0.28	0.15	0.18	0.20	0.27	<MDL	0.07	<MDL	0.09	<MDL	<MDL	<MDL	0.08	<MDL	<MDL	<MDL	<MDL	<MDL	<MDL	<MDL	<MDL	<MDL	<MDL	<MDL	<MDL	<MDL	<MDL	<MDL	<MDL	<MDL
BaA	0.09	<MDL	0.60	0.28	0.37	0.29	0.48	0.06	0.08	0.06	0.16	0.05	<MDL	0.07	0.13	<MDL	<MDL	<MDL	0.10	0.07	0.06	<MDL	<MDL	<MDL	<MDL	<MDL	N.D.	<MDL	<MDL	<MDL	<MDL	<MDL
Chr	0.14	<MDL	1.22	0.71	0.70	0.63	1.11	0.12	0.22	0.15	0.39	0.06	<MDL	0.15	0.32	0.08	<MDL	0.08	0.28	0.12	0.22	<MDL	<MDL	<MDL	0.09	0.13	<MDL	0.07	<MDL	0.07	<MDL	<MDL
Bb+jF	0.16	0.03	1.43	1.04	0.87	0.75	1.50	0.11	0.40	0.21	0.58	0.19	<MDL	0.34	0.52	0.12	0.05	0.12	0.40	0.26	0.29	<MDL	<MDL	0.13	0.08	0.17	0.04	0.12	<MDL	0.09	<MDL	<MDL
BkF	0.07	<MDL	0.72	0.53	0.46	0.38	0.71	<MDL	0.23	0.09	0.38	<MDL	<MDL	0.17	0.25	0.07	<MDL	0.06	0.17	0.16	0.12	<MDL	<MDL	0.08	<MDL	0.09	<MDL	0.07	<MDL	0.07	<MDL	<MDL
DMBA	N.D.	N.D.	N.D.	N.D.	N.D.	N.D.	N.D.	N.D.	N.D.	N.D.	N.D.	N.D.	N.D.	N.D.	N.D.	N.D.	N.D.	N.D.	N.D.	N.D.	N.D.	N.D.	N.D.	N.D.	N.D.	N.D.	N.D.	N.D.	N.D.	N.D.	N.D.	N.D.
BeP	0.11	<MDL	1.18	0.99	0.76	0.64	1.18	0.08	0.37	0.15	0.52	0.05	<MDL	0.36	0.51	0.10	0.06	0.11	0.29	0.27	0.31	<MDL	<MDL	0.15	0.10	0.20	0.05	0.17	<MDL	0.09	<MDL	<MDL
BaP	0.09	<MDL	0.56	0.45	0.37	0.23	0.49	0.06	0.06	0.13	0.24	0.07	<MDL	0.11	0.26	0.09	<MDL	<MDL	0.20	0.10	0.12	<MDL	<MDL	0.06	<MDL	0.10	<MDL	0.06	<MDL	<MDL	<MDL	<MDL
3MCA	N.D.	N.D.	N.D.	N.D.	N.D.	N.D.	N.D.	N.D.	N.D.	N.D.	N.D.	N.D.	N.D.	N.D.	N.D.	N.D.	N.D.	N.D.	N.D.	N.D.	N.D.	N.D.	N.D.	N.D.	N.D.	N.D.	N.D.	N.D.	N.D.	N.D.	N.D.	N.D.
Ind	0.16	0.04	0.93	0.98	0.80	0.62	1.20	0.12	0.35	0.20	0.53	0.10	<MDL	0.32	0.51	0.12	0.05	0.09	0.28	0.28	0.29	<MDL	<MDL	0.13	0.07	0.15	0.03	0.09	<MDL	0.10	<MDL	<MDL
DahA	<MDL	<MDL	0.08	0.07	0.07	<MDL	0.10	<MDL	<MDL	<MDL	<MDL	<MDL	<MDL	<MDL	<MDL	<MDL	<MDL	N.D.	N.D.	<MDL	<MDL	<MDL	N.D.	N.D.	<MDL	<MDL	<MDL	<MDL	<MDL	<MDL	<MDL	<MDL
BghiP	0.15	<MDL	0.86	0.96	0.74	0.60	1.01	0.11	0.31	0.17	0.52	0.07	<MDL	0.43	0.54	0.11	0.07	0.11	0.30	0.30	0.37	<MDL	<MDL	0.17	0.08	0.19	<MDL	0.15	<MDL	0.11	<MDL	<MDL
DbaiP	N.D.	N.D.	N.D.	N.D.	N.D.	N.D.	N.D.	N.D.	N.D.	N.D.	N.D.	N.D.	N.D.	N.D.	N.D.	N.D.	N.D.	N.D.	N.D.	N.D.	N.D.	N.D.	N.D.	N.D.	N.D.	N.D.	N.D.	N.D.	N.D.	N.D.	N.D.	<MDL
DbahP	<MDL	N.D.	0.03	N.D.	N.D.	<MDL	<MDL	N.D.	N.D.	<MDL	N.D.	N.D.	N.D.	N.D.	N.D.	<MDL	N.D.	N.D.	N.D.	N.D.	N.D.	N.D.	N.D.	N.D.	<MDL	N.D.	N.D.	N.D.	N.D.	N.D.	N.D.	N.D.
DbalP	N.D.	N.D.	N.D.	N.D.	N.D.	N.D.	N.D.	N.D.	N.D.	N.D.	N.D.	<MDL	N.D.	N.D.	N.D.	N.D.	N.D.	N.D.	N.D.	N.D.	N.D.	N.D.	N.D.	N.D.	N.D.	N.D.	N.D.	N.D.	N.D.	N.D.	N.D.	N.D.
SUM	1.18	0.07	13.35	9.14	7.79	6.95	12.25	1.17	2.83	1.76	5.01	1.82	0.00	2.48	4.74	1.07	0.29	0.88	2.91	2.03	2.36	0.04	0.00	0.77	0.65	1.50	0.11	0.90	0.00	0.86	0.05	0.21

Table 12. Concentrations (ng/m^3) of the gaseous 21 PAHs during sampling period.

	WT1	WT2	WT3	WT4	WT5	WT6	WT7	WT8	WT9	WT10	SP1	SP2	SP3	SP4	SP5	SP6	SP7	SP8	SP9	SP10	SP11	SU1	SU2	SU3	SU4	SU5	SU6	SU7	SU8	SU9	SU10	SU11
Flu	3.80	1.44	5.91	3.48	0.48	3.62	6.69	2.10	1.76	2.54	2.77	1.74	0.19	1.00	0.42	0.28	0.50	0.13	0.11	< MDL	0.48	0.15	0.35	0.08	0.22	0.10	0.09	0.16	< MDL	0.61	0.12	0.12
Phe	6.51	4.63	6.75	5.88	0.87	5.50	7.69	3.28	3.63	3.79	4.36	5.85	1.35	6.24	1.89	2.13	3.69	2.25	0.73	1.24	6.45	1.77	4.37	1.52	4.23	3.31	3.75	2.81	0.37	5.59	2.78	2.73
Ant	0.75	0.19	0.30	0.46	< MDL	0.22	0.31	0.09	0.24	0.12	0.17	0.51	< MDL	0.26	< MDL	< MDL	0.15	0.11	< MDL	< MDL	0.15	< MDL	0.08	< MDL	0.10	< MDL	0.25	0.13	< MDL	< MDL	0.29	< MDL
Flt	2.16	1.23	1.76	1.83	0.50	1.50	1.81	0.51	1.34	1.21	1.24	2.25	0.72	2.06	0.52	0.76	0.84	0.57	0.37	0.75	1.73	0.41	1.05	0.44	1.51	1.18	1.91	1.35	0.48	1.35	1.25	0.71
Pyr	1.60	0.99	0.99	1.22	0.30	0.80	1.00	0.21	0.88	0.80	0.72	2.54	0.57	1.94	0.30	0.55	0.76	0.42	0.36	0.57	1.65	0.35	1.03	0.40	1.20	1.17	2.15	1.47	0.47	1.20	1.60	0.93
BcPhe	< MDL	< MDL	< MDL	< MDL	< MDL	< MDL	< MDL	< MDL	< MDL	< MDL	< MDL	< MDL	< MDL	< MDL	< MDL	< MDL	< MDL	< MDL	< MDL	< MDL	< MDL	< MDL	< MDL	< MDL	< MDL	< MDL	< MDL	< MDL	< MDL	< MDL	< MDL	< MDL
BaA	< MDL	0.11	< MDL	< MDL	< MDL	N.D.	< MDL	N.D.	< MDL	< MDL	< MDL	< MDL	< MDL	< MDL	< MDL	< MDL	< MDL	< MDL	< MDL	< MDL	< MDL	< MDL	< MDL	< MDL	< MDL	< MDL	< MDL	< MDL	< MDL	< MDL	< MDL	< MDL
Chr	< MDL	0.16	< MDL	< MDL	< MDL	< MDL	< MDL	N.D.	0.09	< MDL	< MDL	0.08	< MDL	0.19	< MDL	< MDL	< MDL	< MDL	< MDL	< MDL	0.14	< MDL	< MDL	< MDL	0.10	< MDL	0.09	< MDL	< MDL	< MDL	< MDL	< MDL
Bb+jF	< MDL	< MDL	< MDL	< MDL	< MDL	N.D.	N.D.	N.D.	< MDL	N.D.	< MDL	< MDL	< MDL	< MDL	< MDL	< MDL	< MDL	< MDL	< MDL	< MDL	< MDL	< MDL	< MDL	< MDL	< MDL	< MDL	< MDL	< MDL	< MDL	< MDL	< MDL	< MDL
BkF	< MDL	< MDL	< MDL	N.D.	< MDL	N.D.	N.D.	N.D.	< MDL	N.D.	< MDL	< MDL	< MDL	< MDL	< MDL	< MDL	< MDL	< MDL	< MDL	< MDL	< MDL	N.D.	N.D.	N.D.	N.D.	N.D.	N.D.	N.D.	< MDL	N.D.	N.D.	N.D.
DMbA	N.D.	N.D.	N.D.	N.D.	N.D.	N.D.	N.D.	N.D.	N.D.	N.D.	N.D.	N.D.	N.D.	N.D.	N.D.	N.D.	N.D.	N.D.	N.D.	N.D.	N.D.	N.D.	N.D.	N.D.	N.D.	N.D.	N.D.	N.D.	N.D.	N.D.	N.D.	N.D.
BeP	< MDL	< MDL	< MDL	< MDL	< MDL	N.D.	< MDL	N.D.	< MDL	N.D.	< MDL	< MDL	< MDL	< MDL	< MDL	< MDL	< MDL	< MDL	N.D.	< MDL	< MDL	< MDL	N.D.	< MDL	< MDL	< MDL	N.D.	< MDL	< MDL	< MDL	< MDL	N.D.
BaP	N.D.	< MDL	< MDL	N.D.	< MDL	N.D.	N.D.	N.D.	N.D.	< MDL	N.D.	N.D.	< MDL	N.D.	N.D.	N.D.	N.D.	N.D.	< MDL	N.D.	N.D.	< MDL	< MDL	< MDL	< MDL	< MDL	< MDL	< MDL	< MDL	< MDL	< MDL	< MDL
3MCA	N.D.	N.D.	N.D.	N.D.	N.D.	N.D.	N.D.	N.D.	N.D.	N.D.	N.D.	N.D.	N.D.	N.D.	N.D.	N.D.	N.D.	N.D.	N.D.	N.D.	N.D.	N.D.	N.D.	N.D.	N.D.	N.D.	N.D.	N.D.	N.D.	N.D.	N.D.	N.D.
Ind	< MDL	< MDL	< MDL	< MDL	< MDL	N.D.	< MDL	N.D.	N.D.	< MDL	< MDL	< MDL	< MDL	< MDL	< MDL	< MDL	< MDL	< MDL	< MDL	< MDL	< MDL	< MDL	< MDL	< MDL	< MDL	< MDL	< MDL	< MDL	< MDL	< MDL	< MDL	< MDL
DahA	N.D.	N.D.	N.D.	N.D.	< MDL	N.D.	N.D.	N.D.	N.D.	N.D.	N.D.	N.D.	N.D.	N.D.	N.D.	N.D.	N.D.	N.D.	< MDL	< MDL	N.D.	N.D.	N.D.	N.D.	N.D.	N.D.	N.D.	< MDL	N.D.	N.D.	N.D.	N.D.
BghiP	< MDL	< MDL	< MDL	< MDL	< MDL	N.D.	< MDL	N.D.	< MDL	N.D.	< MDL	0.22	< MDL	< MDL	< MDL	< MDL	N.D.	< MDL	< MDL	< MDL	< MDL	< MDL	< MDL	< MDL	< MDL	< MDL	< MDL	< MDL	< MDL	< MDL	< MDL	< MDL
DbaiP	N.D.	N.D.	N.D.	N.D.	N.D.	N.D.	N.D.	N.D.	N.D.	N.D.	N.D.	N.D.	N.D.	N.D.	N.D.	N.D.	N.D.	N.D.	< MDL	N.D.	N.D.	N.D.	N.D.	N.D.	< MDL	N.D.	N.D.	N.D.	N.D.	N.D.	N.D.	N.D.
DbahP	N.D.	N.D.	N.D.	N.D.	< MDL	0.22	N.D.	N.D.	N.D.	N.D.	N.D.	N.D.	N.D.	N.D.	N.D.	N.D.	N.D.	N.D.	< MDL	N.D.	N.D.	N.D.	N.D.	N.D.	N.D.	N.D.	N.D.	N.D.	N.D.	N.D.	N.D.	N.D.
DbalP	N.D.	N.D.	N.D.	N.D.	N.D.	N.D.	N.D.	N.D.	N.D.	N.D.	N.D.	N.D.	N.D.	N.D.	N.D.	N.D.	N.D.	N.D.	N.D.	N.D.	N.D.	N.D.	N.D.	N.D.	N.D.	N.D.	N.D.	N.D.	N.D.	N.D.	N.D.	N.D.
SUM	14.82	8.75	15.71	12.87	2.16	11.65	17.51	6.17	7.95	8.46	9.26	13.19	2.83	11.69	3.14	3.72	5.95	3.47	1.57	2.56	10.61	2.68	6.88	2.43	7.36	5.77	8.24	5.92	1.32	8.75	6.04	4.50

ACKNOWLEDGEMENT

처음 이 학교에 발을 디뎠던 2014 년 2 월이 생각납니다. 많이 설렜고, 많이 긴장되었으며, 무엇이든 할 수 있을 것만 같은 기분이었습니다. 부모님의 보호 아래에서 그저 사랑만 받으며 지내던 저는 20 살이 되면 진짜 어른이 될 수 있다고 생각했습니다. 스스로 정말 하고 싶은 게 무엇인지도 몰랐던 제가 환경공학을 전공하며 막연하게 더 깊은 공부를 하고 싶다고 느꼈을 때, 우리 환경분석화학 연구실에 진학하며 그 꿈을 구체화할 수 있었습니다.

1 년 6 개월 간의 인턴 생활과 2 년 간의 석사 생활을 되돌아보면, 그건 모두 오늘의 항해를 위한 준비였습니다. 어리고 어리숙한 저를 받아 주시고 지도해 주신 최성득 교수님께 감사의 말씀 드리고 싶습니다. 아무것도 모른 채 그저 열정만 가득했던 저를 다듬어 주시고, 학문의 길을 알려주셔서 감사합니다. 교수님의 가르침은 저의 밑바탕이 되어 앞으로 나아갈 인생에서도 나침반이 될 것입니다.

석사졸업논문과 논문발표에 많은 조언을 주신 송창근 교수님과 박상서 교수님께서 감사를 표합니다. 바쁘신 와중에도 꼼꼼히 논평해주셔서 정말 감사했습니다. 교수님들 덕분에 무사히 석사졸업논문과 발표를 마무리 지을 수 있었습니다.

3 년 6 개월의 연구실 생활 동안 너무 좋은 사람들을 많이 만났습니다. 우리는 졸업이라는 출항을 위해 열심히 배우고, 또 배우고, 열띤 토론을 하고, 서로의 생각을 받아들였습니다. 민규 오빠, 성준 오빠, 진우 오빠, 상진 오빠, 호영 오빠, 혜경 언니, 인규, 근우 오빠, 혜지, 손지민 선생님, Nam 언니, Quang 오빠, Tien 오빠, Renato 오빠, 졸업한 지영 언니, 현진 언니, 단비 언니까지. 처음에 입학했을 땐 사회생활의 시작이라고 생각했지만, 막상 떠나려고 보니 아쉬운 것은 가족처럼 소중해졌기 때문입니다. 정말 많은 부분에서 정말 많은 것을 배울 수 있어서 행복한 시간이었습니다. 감사합니다. 각자만의 목표를 꼭 이루기를 기원하겠습니다.

UCRF 환경분석센터 선생님들께도 감사드립니다. 근로 장학 활동으로 시작으로 4 년간 김철수 선생님, 손희식 선생님, 예진 선생님, 그리고 이윤세 선생님 덕분에 실험부터 분석까지 많은 것을 배울 수 있었습니다. 늘 건강하시고 행복하셨으면 좋겠습니다.

그리고 사랑하는 가족들. 세상 모든 사람이 저에게 손가락질해도 마지막의 마지막까지 제 편이 되어주겠다는 당신들의 말은 항상 저를 눈물 나게 합니다. 언젠가 신발장에서

같은 모양의 신발 끈 매듭을 가진 신발들을 보았을 때, 저는 어떠한 소속감을 느꼈습니다. 제가 태어나서 가장 처음 접한 행운은 우리 가족들을 가족으로 만난 것입니다. 사랑한다는 한 마디가 쑥스러워서 말이 길어지네요.

이 논문을 끝으로, 저는 진짜 출항을 합니다. 많은 분이 알려주신 지식과 용기와 응원을 바탕으로 비로소 선착장을 떠날 준비가 되었습니다. 내일은, 내년에는, 10년 뒤에는 제가 어디쯤 있을지 알 수 없습니다. 걱정은 하지 않습니다. 목적지가 없는 항해에는 실패가 없으니까요.

긴 글 읽어주셔서 감사합니다.